Annals of Physics **263**, 1–55 (1998)
Article No. PH975750

The 2-Channel Kondo Model

I. Review of Experimental Evidence for Its Realization in Metal Nanoconstrictions

Jan von Delft* and D. C. Ralph

Laboratory of Atomic and Solid State Physics, Cornell University, Ithaca, New York 14853

R. A. Buhrman

School of Applied and Engineering Physics, Cornell University, Ithaca, New York 14853

S. K. Upadhyay and R. N. Louie

Laboratory of Atomic and Solid State Physics, Cornell University, Ithaca, New York 14853

A. W. W. Ludwig

Physics Department, University of California, Santa Barbara, California 93106

and

Vinay Ambegaokar

Laboratory of Atomic and Solid State Physics, Cornell University, Ithaca, New York 14853

Received March 27, 1997

Certain zero-bias anomalies (ZBAs) in the voltage, temperature and magnetic field dependence of the conductance $G(V, T, H)$ of quenched Cu point contacts have previously been interpreted to be due to non-magnetic 2-channel Kondo (2CK) scattering from near-degenerate atomic two-level tunneling systems (Ralph and Buhrman, 1992; Ralph *et al*., 1994) and hence to represent an experimental realization of the non-Fermi-liquid physics of the $T=0$ fixed point of the 2-channel Kondo model. In this, the first in a series of three papers (I, II, III) devoted to 2-channel Kondo physics, we present a comprehensive review of the quenched Cu ZBA experiments and their 2CK interpretation, including new results on ZBAs in constrictions made from Ti or from metallic glasses. We first review the evidence that the ZBAs are due to electron scattering from stuctural defects that are not static, but possess internal dynamics. In order to distinguish between several mechanisms proposed to explain the experiments, we then analyze the scaling properties of the conductance at low temperature and voltage and extract from the data a universal scaling function $\Gamma(v)$. The theoretical calculation of the corresponding scaling function within the 2CK model is the subject of papers II and III. The main conclusion of our work is that the properties of the ZBAs, and most notably their scaling behavior, are in good agreement with the 2CK model and clearly different from several other proposed mechanisms.

* Present address: Institut für Theoretische Festkörperphysik, Universität Karlsruhe, D-76128 Karlsruhe, Germany.

0003-4916/98 $25.00

Contents.

1. INTRODUCTION

The study of systems of strongly correlated electrons that display non-Fermi-liquid behavior has attracted widespread interest in recent years, fueled in part by their possible relevance to heavy-fermion compounds [3–5] and high-T_c superconductivity materials [6–8]. On the theoretical front, one of the consequences was a renewed interest in various multi-channel Kondo models, some of which were predicted by Nozières and Blandin [9] to contain non-Fermi-liquid physics. Some of the most recent advances were made by Affleck and Ludwig (AL) (see [10] and references therein), who developed an exact conformal field theory (CFT) solution for the $T=0$ fixed point of the multichannel Kondo models. On the experimental front, an experiment performed by two of us (RB) [1, 11], that investigated certain zero-bias anomalies (ZBAs) in the conductance of quenched Copper nanoconstrictions, has emerged as a potential experimental realization of the 2-channel Kondo (2CK) model and the corresponding non-Fermi-liquid physics [2, 12–14]. Although criticisms of the 2CK interpretation [15, 16] and alternative mechanisms for the ZBAs have been offered [17, 18], the 2CK scenario has recently received important additional support from experimental results on ZBAs in constrictions made from Titanium [19] and from metallic glasses [20, 21].

In a series of three papers (I, II, III) we shall present a detailed analysis of these ZBA experiments and their 2CK interpretation. The present paper (I) is a comprehensive review of the ZBA experiments that attempts to integrate all experimental results on the quenched Cu, Ti and metallic glass constrictions into a coherent picture (while postponing all formal theoretical developments to papers II and III). Paper II contains a calculation of the non-equilibrium conductance through a nanoconstriction containing 2CK impurities, which is compared with the Cu experiments. Paper III, which is the only paper of the three that requires knowledge of AL's conformal field theory solution of the 2CK model, describes a bosonic reformulation [22] of their theory that is considerably simpler than those used previously and is needed to derive certain key technical results used in paper II.

Let us begin by briefly summarizing the quenched Cu ZBA experiments and how they inspired the theoretical work presented in papers II and III.

RB used lithographic techniques to manufacture quenched Cu constrictions of diameters as small as 3 nm (see Fig. 1), and studied the conductance $G(V, T, H)$ through the so-called nanoconstriction (or point contact) as a function of voltage (V), temperature (T) and magnetic field (H). Their constrictions were so small that they were able to detect electron scattering at the level of individual impurities or defects in the constriction. Since the energy dependence of the scattering rate can be extracted from the voltage dependence of the conductance, such an experiment probes the actual electron-impurity scattering mechanism.

For very small eV/k_B and T ($<5K$), RB observed non-ohmic ZBAs in the V- and T-dependence of the conductance signals of unannealed, ballistic nanoconstrictions. The qualitative features of these anomalies (such as their behavior in a magnetic field, under annealing and upon the addition of static impurities), which are reviewed in detail in the present paper, lead to the proposal [1] that the ZBAs are caused by a special type of defect in the nanoconstrictions, namely two-level systems (TLSs). This proposal has recently received strong support from a number of subsequent, related experiments (briefly reviewed in Section VII) by Upadhyay *et al.* on Ti constrictions [19] and by Keijsers *et al.* on metallic-glass constrictions [20, 21].

There are at least two theories for how TLSs can cause ZBAs in nanoconstrictions. In the first, based on Zawadowski's *non-magnetic Kondo model* [23, 24], the interaction between TLSs and conduction electrons is described, at sufficiently low energies, by the 2CK model (reviewed in Appendix B of paper II), leading to an energy dependent scattering rate and hence a ZBA. In the second, Kozub and Kulik's theory of *TLS-population spectroscopy* [17, 18], the ZBA is attributed to a V-induced non-equilibrium occupation of the upper and lower energy states of the TLSs (see Appendix A.3).

Though the two theories make quite similar predictions for the shape of the ZBA, they make different predictions for the V/T-scaling behavior of $G(V, T)$. Whereas Kozub and Kulik's theory predicts that $G(V, T)$ does not obey any V/T-scaling relation at all, the 2CK scenario predicts [2] that in the regime $T \ll T_K$ and $eV \ll k_B T_K$ (where T_K is the Kondo temperature), the conductance $G(V, T)$ should obey a scaling relation of the form

$$\frac{G(V, T) - G(0, T)}{T^{\alpha}} = F(eV/k_B T), \tag{1}$$

where $F(x)$ is a sample-dependent scaling function. Moreover, AL's CFT solution of the 2CK problem suggested that by scaling out non-universal constants, it should be possible to extract from $F(x)$ a *universal* (i.e. sample-independent) scaling curve $\Gamma(x)$, and that the conductance exponent α should have the universal non-Fermi-liquid value $\alpha = \frac{1}{2}$, in striking contrast to the usual Fermi-liquid value [25] of $\alpha = 2$. Since no calculation had been provided in Ref. [2] to support the statement that $\alpha = \frac{1}{2}$, its status up to now has been that of an informed guess rather than a definite prediction, a situation that is remedied in papers II and III.

A detailed scaling analysis [2] showed that the data of RB indeed do obey the above scaling relation, with $\alpha = 0.5 \pm 0.05$. It should be emphasized that the verification of scaling was a very significant experimental result: firstly, the scaling relation (1), by combining the V- and T-dependence of $G(V, T)$ for arbitrary ratios of V/T, contains much more information than statements about the separate V- or T-dependence would; and secondly, an accurate experimental determination of the scaling exponent α is possibly only by a scaling analysis of all the data (for a detailed review of this central ingredient of the data analysis, see Section VI). Accurate knowledge of α is very important, since α succinctly characterizes the low-energy critical properties of the physics, enabling one to eliminate many otherwise plausible candidate theories for the ZBA (such as that by Kozub and Kulik).

The experimental value for α agrees remarkably well with the CFT prediction of $\alpha = \frac{1}{2}$; furthermore, the scaling curve $\Gamma(x)$ is indeed the same for all three samples studied in detail by RB, in accord with the CFT expectation that it should be universal and hence sample-independent. Thus, this result considerably strenghtened the case for the 2CK interpretation of the RB experiment, within which the experimental demonstration that $\alpha = \frac{1}{2}$ is, remarkably, equivalent to the direct observation of non-Fermi-liquid physics.

Nevertheless, this scaling behavior can conceivably also be accounted for by some other theory. Indeed, Wingreen, Altshuler and Meir [15](a) have pointed out that an exponent of $\alpha = \frac{1}{2}$ also arises within an alternative interpretation of the experiment, based not on 2CK physics but the physics of disorder. (We believe that this interpretation is in conflict with other important experimental facts, see Section A.1).

It is therefore desirable to develop additional quantitative criteria for comparing experiment to the various theories. One possible criterion is the scaling function $\Gamma(x)$. A very stringent quantitative test of any theory for the RB experiment would therefore be to calculate the universal scaling function $\Gamma(x)$, which should be a fingerprint of the theory, and compare it to experiment. Papers II and III are devoted to this task: $\Gamma(x)$ is calculated analytically within the framework of the 2CK model and its exact CFT solution by AL, and the results are compared to the RB experiment. When combined with recent numerical results of Hettler *et al.* [12], agreement with the experimental scaling curve is obtained, thus lending further quantitative support to the 2CK interpretation for the Cu constrictions.

The main conclusion of our work is that the 2CK interpretation can qualitatively and quantitatively account for all the scaling properties of the conductance measured in the ZBAs of Cu point contacts. The Ti and metallic glass results add further evidence in support of the 2CK interpretation, as opposed to other proposed mechanisms. However, we shall note that the 2CK model does not account for two phenomena observed in the quenched Cu samples. Firstly, the magnetic field dependence of the low-bias conductance is rather strong (the 2CK explanation for the field dependence that was offered in Ref. [2] does not seem to survive closer scrutiny, as discussed in Appendix B). Secondly, in many (but not all) Cu constrictions the conductance undergoes very sudden transitions at certain voltages V_c [11, 26] (see (Cu.9) of Section IV) if T and H are sufficiently small. These voltages can be rather large (V_c

typically ranges between 5 and 20 mV), implying that some new, large energy scale is involved. These two phenomena are not generic to TLS-induced ZBAs, however, since they are observed neither in metallic-glass constrictions nor in Ti constrictions, which in fact conform in all respects to what is expected for 2CK physics. We shall suggest that the two phenomena involve (as yet poorly understood) "high-energy" physics associated with the strongly-interacting system of electrons and atomic tunneling centers. Such physics is beyond the scope of the existing 2CK model and its CFT treatment, which deals only with the "low-energy" aspects of the problem.

Paper I is organized as follows: In Section II we describe the fabrication and characterization of nanoconstrictions, and summarize some elements of ballistic point contact spectroscopy in Section III. In Section IV we summarize the main experimental facts associated with the ZBA in the Cu samples, which we state in the form of nine properties, (Cu.1) to (Cu.9). The 2CK interpretation is presented in Section V, where its assumptions are summarized and critically discussed. Section VI contains a scaling analysis of the $G(V, T)$ data at $H = 0$. The related ZBA experiments on Ti and metallic-glass nanoconstrictions are discussed in Section VII. Finally, we summarize the results and conclusions of this paper in Section VIII. Appendix A describes experimental arguments for ruling out a number of conceivable explanations for the ZBA that could come to mind as possible alternatives to the 2CK scenario. In Appendix B we discuss possible sources of magnetic field dependence in the 2CK scenario, concluding it is essentially H-independent.

2. THE NANOCONSTRICTION

A schematic cross-sectional view of a typical nanoconstriction (often also called a *point contact*) is shown in Fig. 1. The device is made in a sandwich structure. The middle layer is an insulating Si_3N_4 membrane. This contains in one spot a bowl-shaped hole, which just breaks through the lower edge of the membrane to form a very narrow opening, as small as 3 nm in diameter. This opening is so small that the resistance signal, measured between the top and bottom of the structure, is completely dominated by the region within a few constriction radii of the opening. Hence the resistance is sensitive to scattering from single defects in the constriction region.

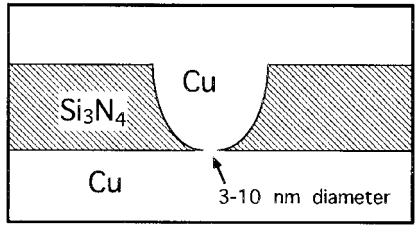

Fig. 1. Cross-sectional schematic of a metal nanoconstriction. The hole at the lower edge of the Si_3N_4 is so small that this region completely dominates the resistance of the device.

To obtain the bowl-shaped hole in a Si_3N_4 membrane, electron beam lithography and reactive ion etching are used in a technique developed by Ralls [27] (the details relevant to the present experiments are described in Ref. [11], Section 2.2). In ultra-high vacuum ($<2\times10^{-10}$ torr) and at room temperature the membrane is then rotated to expose both sides while evaporating metal to fill the hole (thus forming a metallic channel through the constriction) and coat both sides of the membrane. A layer of at least 2000 $\AA$ of metal (Cu or Ti in the work described below) is deposited on both sides of the membrane to form clean, continuous films, and then the devices are quenched (see property (Cu.1) in Section IV).

3. BALLISTIC POINT CONTACT SPECTROSCOPY

A constriction is called *ballistic* if electrons travel ballistically through it, along semi-classical, straight-line paths between collisions with defects or the walls of the constriction. This occurs if two conditions are fulfilled: Firstly, it must be possible to neglect effects due to the diffraction of electron waves, i.e. one needs $1/k_F \ll a$, where $a =$ constriction radius. Secondly, the constriction must be rather clean (as opposed to disordered): an electron should just scatter off impurities once or twice while traversing the hole. One therefore needs $a \ll l$, where l is the electron mean free path.

The quenched Cu ZBA-devices of RB reasonably meet both conditions: firstly, for Cu $1/k_F \simeq 0.1$ nm, whereas a is of order 2–8 nm [as determined from the Sharvin formula for the conductance, Eq. (3)]. Secondly, for clean, annealed devices $l \sim 200$ nm (as determined from the residual bulk resistivity). For devices containing structural defects, l is reduced to about $l \gtrsim 30$ nm [see (Cu.4)], which is still about twice the constriction diameter. Thus, we shall henceforth regard the quenched Cu ZBA-devices as ballistic constrictions.

Some aspects of the theory of transport through ballistic constrictions [28, 29] are reviewed in Appendix A of paper II. Here we merely summarize the main conclusions.

The differential conductance has the general form

$$G(V) \equiv \left|\frac{dI(V)}{dV}\right| = G_o + \Delta G(V). \tag{2}$$

The constant G_o, the so-called Sharvin conductance, arises from electrons that travel ballistically through the hole without scattering. Sharvin showed that for a round hole,

$$G_o = a^2 e^2 m \varepsilon_F/(2\pi h^3), \tag{3}$$

where a is the radius of the hole, and hence the measured value of G_o can be used to estimate the size of the constriction.

Any source of scattering in the constriction that backscatters electrons and hence prevents them from ballistically traversing the hole gives rise to a backscattering correction ΔG. If the electron scattering rate $\tau^{-1}(\varepsilon)$ is energy-dependent, $\Delta G(V)$ is voltage dependent. In fact, one of the most important characteristics of ballistic

nanoconstrictions is that the energy dependence of $\tau^{-1}(\varepsilon)$ can be directly extracted from the voltage dependence of $\Delta G(V)$, which implies that ballistic nanconstrictions can be used to do spectroscopy of electron-defect scattering.

If, for example, the voltage is large enough to excite phonons (>5mV for Cu), the I-V curve is dominated by electron-phonon scattering. In this case, it can be shown that at $T=0$, $\Delta G(V) = -(4e^2m^2v_Fa^3/3\pi h^4)\,\tau^{-1}(eV)$, where $\tau^{-1}(\varepsilon') \equiv \int_0^{\varepsilon'} d\varepsilon\, \alpha^2F_p(\varepsilon)$ is the relaxation rate for an electron at energy ε' above the Fermi surface. Thus, due to phonon-backscattering processes, the conductance of any point contact drops markedly at voltages large enough to excite phonons [$V>5$ meV for Cu, see Fig. 2(a)]. Furthermore, the function $\alpha^2F_p(eV)$, the so-called *point contact phonon spectrum*, can be directly obtained from $\partial_V \Delta G(V)$. For any clean, ballistic Cu nanoconstriction, $\partial_V \Delta G(V)$ should give the same function $\alpha^2F_p(eV)$, characteristic

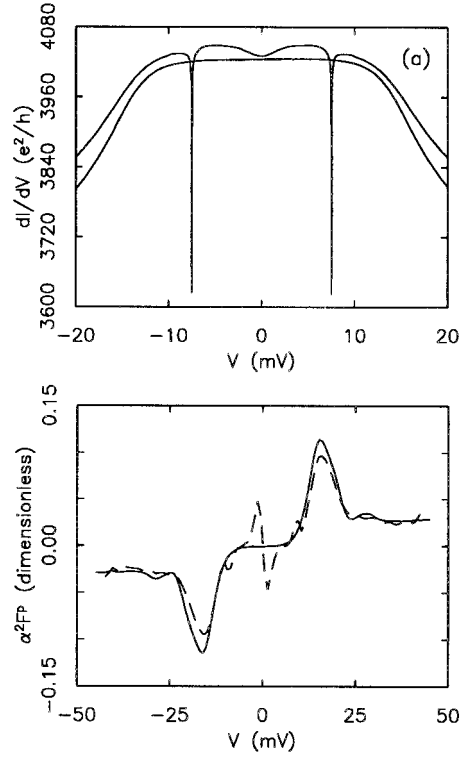

Fig. 2. A typical conductance curve for a constriction containing structural defects: (a) The upper curve, showing a dip in conductance at $V=0$ and voltage-symmetric spikes, is the differential conductance for an unannealed Cu sample at 4.2 K. The lower curve shows the conductance of the same device at 4.2 K, after annealing at room temperature for 2 days. The curves are not artificially offset; annealing changes the overall conductance of the device by less than 0.5%. (b) Point contact phonon spectrum at 2 K for the device before anneal (dashed line) and after anneal (solid line).

of the phonon spectrum, and indeed nanoconstriction measurements thereof agree with other determinations of $\alpha^2 F_p$. However, the amplitude of the phonon-induced peaks is reduced dramatically if there is significant elastic scattering due to defects or impurities in the constriction region, as has been modeled theoretically [30] and demonstrated experimentally [31]. Therefore, comparing the point contact phonon spectrum of a given point contact to the reference spectrum of a clean point contact provides an important and reliable tool for determining whether the point contact is clean or not.

For voltages below the phonon threshold ($V < 5\text{mV}$ for Cu), the V-dependence of $\Delta G(V)$ is due to scattering off defects. For a set of defects at positions $\vec{R}_i$, with an isotropic, elastic, but energy-dependent scattering rate $\tau^{-1}(\varepsilon)$, the backscattering conductance has the form [14]

$$\Delta G(V) = -(\tau(0)\, e^2/h) \int_{-\infty}^{\infty} d\omega [-\partial_\omega f_o(\hbar\omega)] \times \sum_i b_i \tfrac{1}{2} [\tau^{-1}(\hbar\omega - \tfrac{1}{2} eV a_i^+) + \tau^{-1}(\hbar\omega - \tfrac{1}{2} eV a_i^-)]. \tag{4}$$

We factorized out the constant $\tau(0)\, e^2/h$ to ensure that ΔG has the correct dimensions and order of magnitude. We assume that the resistance contribution from each defect may be calculated independently—that is, that quantum interference for electrons scattering from multiple defects may be ignored. The a_i and b_i are (unknown) constants of order unity that characterize all those details of scattering by the ith impurity that are energy-independent and of a sample-specific, geometrical nature. The b_i account for the fact that the probability that an electron will or will not traverse the hole after being scattered off the ith impurity depends on the position of the impurity relative to the hole. The a_i account for the fact that impurities that are at different positions $\vec{R}_i$ in the nanoconstriction feel different effective voltages (because the amount by which the non-equilibrium electron distribution function at $\vec{R}_i$ differs from the equilibrium Fermi function f_o depends on $\vec{R}_i$).

In spite of the presence of the many unknown constants a_i, b_i, we shall see that it is nevertheless possible to extract general properties of $\tau^{-1}(\varepsilon)$ from the measured $\Delta G(V, T)$ data. For example, from Eq. (4) one can deduce that if

$$\tau^{-1}(\varepsilon, T) - \tau^{-1}(0, T) \propto \begin{cases} \ln[\max(T, \varepsilon)], \\ T^\alpha \tilde{\Gamma}(\varepsilon/T), \end{cases}$$

$$\text{then} \quad \Delta G(V, T) \propto \begin{cases} \ln[\max(T, V)], \\ T^\alpha F(V/T), \end{cases} \tag{5}$$

where $\tilde{\Gamma}$ and F are scaling functions.

4. EXPERIMENTAL FACTS FOR QUENCHED CU SAMPLES

In this section we summarize the experimental facts relevant to the ZBA in quenched Cu samples. Our interpretation of these facts is postponed to later sections, where some of them will be elaborated upon more fully, and where most of the figures quoted below can be found.

The phenomenon to be studied is illustrated by the upper differential conductance curve in Fig. 2. Its three essential features are the following: Firstly, the differential conductance shows a drop for $|V| > 5$ mV, due to the excitation of phonons, a process which is well understood (see Section III). Secondly, there are sharp voltage-symmetric conductance spikes at somewhat larger voltages (V_c), called *conductance transitions* in Ref. [1, 32], because in the DC conductance they show up as downward steps with increasing V (see Figure 13 below). Some of their complex properties are listed in point (Cu.9) below.

Thirdly, the conductance has a voltage-symmetric dip near $V = 0$; this is the so-called *zero-bias anomaly* (ZBA). As a sample is cooled, the temperature at which the zero-bias features become measurable varies from sample to sample, ranging from 10 K to 100 mK. This paper is concerned mainly with the regime $V < 5$ mV dominated by this ZBA.

The ZBA is a very robust phenomenon. For decades it has been observed, though not carefully investigated, in mechanical "spear and anvil" point contacts made from a variety of materials, see e.g. [33]. Even the dramatic conductance transitions have probably been seen in early ZBA experiments [28], though their presence had not been emphasized there.[1]

The advent of the mechanically very stable nanoconstrictions employed by RB allowed a detailed systematic study of the ZBA. Their findings are discussed at length in [11] and [32]. We summarize them in the form of 9 important properties of the ZBA in quenched Cu nanoconstrictions:

(Cu.1) *Quenching*: ZBAs and conductance transitions [Fig. 2(a)] are found only in *quenched* Cu samples, i.e. samples that are cooled to cryogenic temperatures within hours after being formed by evaporation. They are found in about 50% of such samples, and in a variety of materials, such as Cu, Al, Ag and Pt. Cu was used in the samples discussed below).

(Cu.2) *Amplitude*: Typical values for $G(V = 0)$ vary from 2000 to 4000 e^2/h. The anomaly is only a small feature on a very big background conductance: its amplitude $[G_{max} - G(V = 0)]$ varies from sample to sample, from a fraction of e^2/h to as large as $70e^2/h$ at 100 mK. It's sign is always the same, with $G(V, T)$ increasing from $G(0, T_o)$ as V or T are increased. The sample ($\#1$ in Fig. 7) showing best scaling (see (Cu.6) below) had a maximum ZBA amplitude of about $20e^2/h$.

[1] For example, Fig. 3C of [28] shows a d^2/dV^2 spectrum with sharp signals, more or less symmetric about zero, that are consistent with being derivatives of spikes in the dI/dV conductance curve. Note that these signals are too sharp to be spectroscopic signals smeared by kT, but are indicative of abrupt transitions.

(Cu.3) *Annealing*: (a) After annealing at room temperature for several days, the ZBA and conductance spikes disappear, and the conductance curve looks like that of a completely clean point contact [see lower curve in Fig. 2(a)].

(b) Nevertheless, such annealing changes the total conductance by not more than 1% or 2% (both increases and decreases have been observed), indicating that the overall structure of the constriction does not undergo drastic changes.

(c) Upon thermal cycling, i.e. brief (several minutes) excursions to room temperature and back, the amplitude of the ZBA and the position V_c of the conductance transitions change dramatically and non-monotonically [see Fig. 3(a)]. The complexity of this behavior suggests that the thermal cycling is causing changes in the position of defects within the constriction, and that the ZBA is very sensitive to the precise configuration of the defects.

(Cu.4) *Effect of disorder*: (a) If static disorder is intentionally introduced into a nanoconstriction by adding 1% or more of impurity atoms such as Au to the Cu during evaporation, the zero-bias conductance dip and conductance spikes *disappear completely* [see Fig. 3(b)]. Likewise, the signals are absent in samples for which water is adsorbed onto the Si_3N_4 surface before metal deposition (the standard sample fabrication procedure therefore involves heating the sample to $\sim 100°C$ in vacuum, or exposing it for several hours to ultraviolet light in vacuum, before the final metal evaporation is done).

(b) When a strongly disordered region is created near the constriction (by electromigration: a high bias (100–500 mV) is applied at low temperatures so that Cu atoms are moved around, a method controllably demonstrated in [27, 34, 35]), the conductance shows no ZBA either, but instead small-amplitude, voltage-dependent (but aperiodic) conductance fluctuations at low voltage [see Fig. 3(c), (d)]. That these are characteristic of strongly disordered constrictions and can be interpreted as universal conductance fluctuations due to quantum interference, was established in a separate investigation [36], [11, Chapter 4], [37].

(Cu.5) *Phonon spectrum*: For quenched samples, in the point contact phonon spectrum the longitudinal phonon peak near 28 mV is not well-defined, and the total amplitude of the spectrum is smaller by about 15% than after annealing. After annealing, the longitudinal phonon peak reappears and the spectrum corresponds to that of clean ballistic point contacts. Both these differences indicate (see p. 7) that the elastic mean free path l in the annealed samples is somewhat longer than in the quenched samples. From the phonon spectrum of the latter, l can be estimated (see Section II) to be $l \gtrsim 30$ nm [for the sample shown in Fig. 2(a)], still more than about twice the constriction diameter for that device. Note also that the point contact phonon spectrum for a quenched device [Fig. 2(b)] is qualitatively very different from that of a strongly disordered constriction [Fig. 3(d)]. These facts, viewed in conjunction with (Cu.3b) and (Cu.4c), imply that the Cu constrictions displaying ZBAs are still rather clean and ballistic.

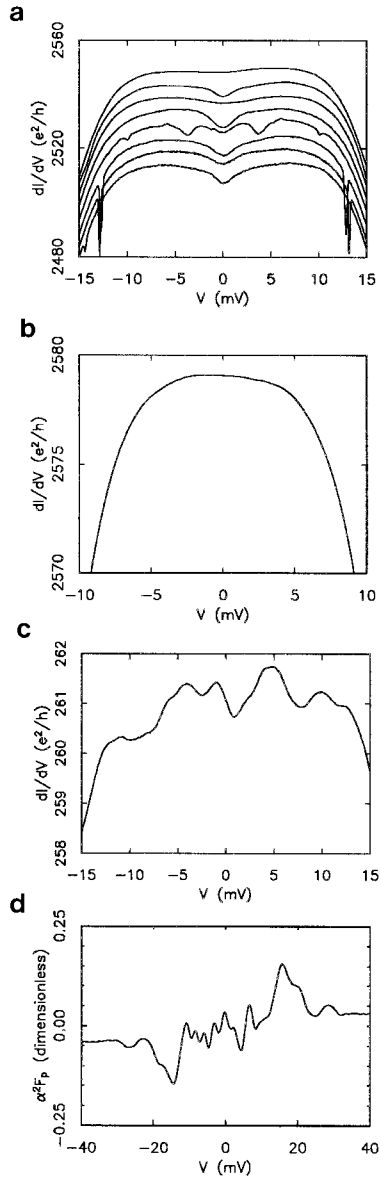

Fig. 3. (a) Differential conductance versus voltage at 4.2 K for a Cu sample which underwent repeated thermal cycling [11]. The time sequence runs from the bottom curve to the top. Curves are artificially offset. The first 2 excursions were to 77 K, the next 5 to room temperature. (b) Differential conductance for a Cu sample intentionally doped with 6% Au. Static impurities reduce the electronic mean free path but completely eliminate the zero-bias anomaly of interest to us. (c) Differential conductance and (d) point contact spectrum for a Cu device at 1.8 K in which disorder has been created by electromigration (which means that a high bias (100–500 mV) has been applied at low temperatures so that Cu atoms moved around).

(Cu.6) *V/T scaling* (to be established in detail in Section VI): (a) At $H=0$, the conductance obeys the following scaling relation if both $V<V_K$ and $T<T_K$, but for arbitrary ratio $v=eV/k_BT$:

$$\frac{G(V,T)-G(0,T)}{T^{\alpha}}=F(v). \tag{6}$$

Relation (6) allows a large number of data curves to be collapsed onto a single, sample-dependent scaling curve [e.g. see Figs. 8(a) and 8(b) below]. The departure of individual curves from the low-T scaling curve in Figs. 8(a) and 8(b) indicates that V or T has surpassed the crossover scales V_K or T_K. From the data, these are related roughly by $eV_K=2k_BT_K$, with T_K in the range 3 to 5 K.

(b) $F(v)$ is a sample-dependent scaling function with the properties $F(0)\neq 0$ and $F(v)\propto v^{\alpha}$ as $v\to\infty$, and the scaling exponent is found to have the value $\alpha=0.5\pm 0.05$.

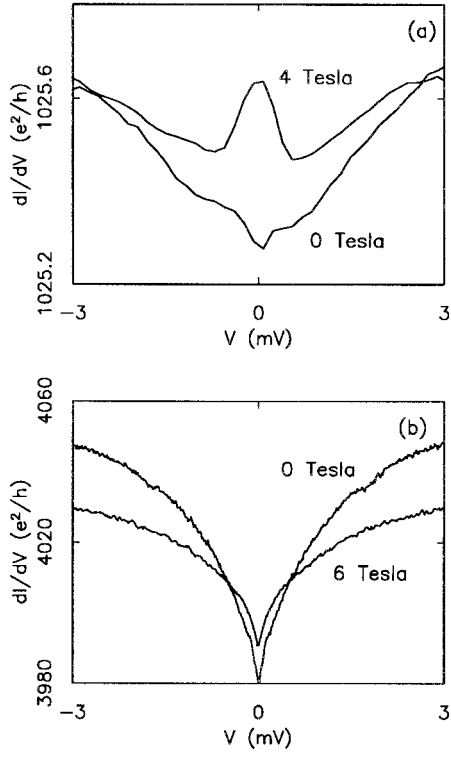

Fig. 4. (a) Conductance signals for 500 ppm magnetic Mn impurities in Cu at 100 mK, showing Zeeman splitting in an applied magnetic field. (b) The ZBA signals from quenched Cu samples exhibit no Zeeman splitting, demonstrating that they are not due to a magnetic impurity. However, the shape and amplitude of the ZBA does depend on magnetic field.

(c) By scaling out sample-dependent constants, it is possible to extract from $F(v)$ a "universal" scaling function $\Gamma(v)$ [shown in Fig. 11(b) below]. $\Gamma(v)$ is universal in the sense that it is indistinguishable for all three devices for which a scaling analysis was carried out (they are called sample 1, 2 and 3 below).

(Cu.7) *Logarithms*: For V or T beyond the cross-over scales V_K or T_K, $G(V, T)$ deviates markedly from the scaling behavior of (Cu.6) and behaves roughly logarithmically: For $H=0$ and fixed, small T, the conductance goes like $\ln V$ for $V > V_K$ [Fig. 5(a)]; similarly, for $H=V=0$ and $T > T_K$, the conductance goes like $\ln T$ [Fig. 5(b)].

(Cu.8) *Magnetic field*: (a) When a magnetic field (of up to 6 T) is applied, the amplitude of the ZBA in Cu devices decreases [see Fig. 4(b)]. The change in amplitude can be as large as $24\, e^2/h$ if H changes from 0 to 6 T. For sufficiently small H (<1T), at fixed T and $V=0$, the magnetoconductance roughly follows $G(H, T) \propto |H|$ (see Fig. 14 below). However, the available data is insufficient to

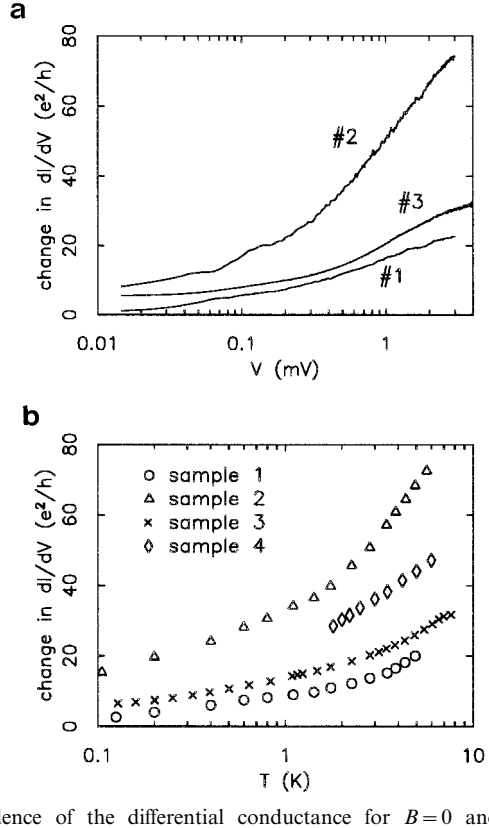

Fig. 5. (a) V-dependence of the differential conductance for $B=0$ and $T=100$ mK, for three different samples, #1, #2, #3, (b) T-dependence of the conductance for $B=0$ and $V=0$ for the three samples of (a), and a fourth.

establish linear behavior beyond doubt, and, for example, would also be compatible with a $|H|^{1/2}$-dependence.

(b) The ZBA dip undergoes no Zeeman-splitting in H, in constrast to the Zeeman splitting that *is* found for devices intentionally doped with magnetic impurities such as Mn [see Fig. 4(a)].

(Cu.9) *Conductance transitions*: (a) Voltage-symmetric conductance transitions (spikes in the differential conductance at certain "transition voltages" V_c, see Fig. 2) occur only in quenched point contacts that show ZBAs, but occur in at least 80% of these. The spikes disappear under annealing, just as the ZBA does (Cu.3a).

(b) (i) A single sample can show several such conductance transitions (up to 6 different V_cs have been observed in a single sample). (ii) If T and H are small (say $T \lesssim 1\text{K}$, $H \lesssim 0.5\text{T}$), V_c is typically rather large, with typical values ranging between 5 and 20 mV, well above the typical voltages associated with the ZBA (i.e. $V_c > V_K$). The spikes have a very complex behavior as a function of temperature (T) and magnetic field (H), including (iii) a hysteretic V-dependence, (iv) a bifurcation of single spikes into two separate ones (V_{c1}, V_{c2}) when $B \neq 0$ (Fig. 12), (v) the H-dependent motion of the spike positions $V_c(H) \to 0$ when H becomes sufficiently large (Figs. 12, 13), and (vi) a very rapid narrowing of the peaks with decreasing T. They are described at length, from a phenomenological point of view, in Ref. [32].

Any theory that purports to explain the ZBA in Cu constrictions must be consistent with all of the above experimental facts. An extention of this list to include the results of the recent related ZBA experiments by Upadhyay *et al.* on Ti constrictions and by Keijsers *et al.* [21] on metallic-glass constrictions is presented in Section VII.

In the next section, we shall argue that the 2CK scenario provides the most plausible interpretation of the above experimental facts. A number of alternative explanations for the ZBA that could come to mind are discussed in Appendix A, but all are found to be in conflict with some of the above facts.

V. THE 2-CHANNEL KONDO (2CK) INTERPRETATION

In this section, we develop the 2CK interpretation of the ZBAs in quenched Cu constrictions. *It attributes the ZBA to the presence in the constriction region of dynamical structural defects, namely TLSs, that interact with conduction electrons according to the non-magnetic Kondo model, which renormalizes at low energies to the non-Fermi-liquid regime of the 2CK model.* We begin by briefly recalling in Section V.A some properties of two-level systems (or slightly more generally, dynamical two-state systems) in metals. Successes and open questions of the 2CK scenario are discussed in subsections V.B and V.C, respectively, and its key assumptions are listed, in the form of a summary, in subsection V.D.

A. *Two-State Systems*

A dynamical two-state system (TSS), is an atom or group of atoms that can move between two different positions inside a material [38]. In the absence of interactions, its behavior is governed by a double-well potential, generically depicted in Fig. 6, with asymmetry energy Δ_z, tunneling matrix element Δ_x. The corresponding Hamiltonian is

$$H_{TSS} = \tfrac{1}{2}(\Delta_z \tau^z + \Delta_x \tau^x), \tag{7}$$

where τ^x and τ^z are Pauli matrices acting in the two-by-two Hilbert space spanned by the states $|L\rangle$ and $|R\rangle$, describing the fluctuator in the left or right well.

Depending on the parameters of the potential, the atom's motion between the potential wells is classified as either slow, fast or ultrafast, with hopping rates $\tau^{-1} < 10^8 s^{-1}$, $10^8 s^{-1} < \tau^{-1} < 10^{12} s^{-1}$ or $\tau^{-1} > 10^{12} s^{-1}$, respectively [39]. *Slow* two-state systems, called *two-state fluctuators*, have large barriers and neglibibly small Δ_x, and the motion between wells occurs due to thermally activated hopping or incoherent quantum tunneling. *Fast* two-state systems have sufficiently small barriers and sufficiently large Δ_x that *coherent tunneling* takes place back and forth between the wells. Such a system is known as a *two-level tunneling system* (TLS), because its physics is usually dominated by its lowest two eigenstates (even and odd linear combinations of the lowest-lying eigenstates of each separate well), whose eigenenergies differ by $\Delta = (\Delta_z^2 + \Delta_x^2)^{1/2}$. *Ultra-fast* two-state systems have such a large Δ_x that Δ too becomes very large, so that at low temperatures only the lowest level governs the physics.

1. *Slow Fluctuators*

The fact that two-state systems in metal nanoconstrictions can influence the conductance was demonstrated by Ralls and Buhrman [34, 35, 37], who observed so-called telegraph signals in *well*-annealed devices (at rather high temperatures of 20-150 K). These are slow, time-resolved fluctuations (fluctuation rates of about

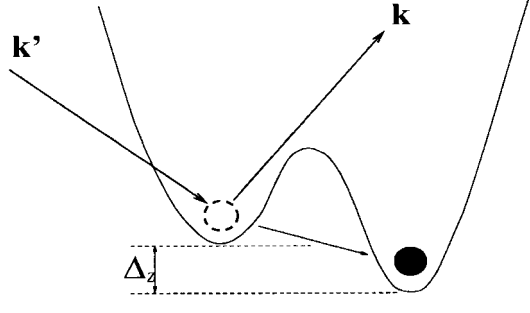

Fig. 6. A generic two-level-system, with (bare) energy asymmetry Δ_z and tunneling rate Δ_x. An electron-assisted tunneling event is depicted: an electron scatters of the TLS and induces the atom to tunnel.

$10^3 s^{-1}$) of the conductance between two (or sometimes several) discrete values, differing by fractions of e^2/h, which can be attributed to the fluctuations of a *slow* two-state fluctuator in the constriction region.

Such telegraph signals were also observed by Zimmerman *et al.* [40, 41], who studied the conductance of polychrystalline Bi films, a highly disordered material with presumably large numbers of two-state systems. They were able to measure the parameters of individual slow fluctuators directly, finding values for the asymmetry energy Δ_z ranging from as little as 0.08 K to about 1 K. They also demonstrated that in a disordered environment the asymmetry energy of a TLS is a random, non-monotonic function of the magnetic field, $\Delta_z = \Delta_z(H)$ (as predicted earlier in Ref. [42]), and hence can be "tuned" at will by changing H. The reason is, roughly, that Δ_z depends on the difference $\delta\rho = \rho_L - \rho_R$ between the local electron densities at the two minima of the TLS potential. Due to quantum interference effects that are amplified by the presence of disorder, changes in H can induce random changes in $\delta\rho$ and hence also in Δ_z.

Unfortunately, experiments on *slow* fluctuators do not yield any direct information on the parameters to be expected for fast ones, since their parameters fall in different ranges.

2. *Two-Level Systems*

Fast fluctuators or TLSs presumably have the same microscopic nature and origin as slow fluctuators, being composed of atoms or small groups of atoms which move between two metastable configurations, but with much lower barriers. Therefore, they anneal away quicker than slow fluctuators, which is why they were not seen in the above-mentioned Ralls–Buhrman experiments on well-annealed samples [11, p. 265]. Also, whereas slow fluctuators "freeze out" as T is lowered (which is why they don't play a role in the ZBA regime of $T < 5$ K), at low T fast fluctuators continue to undergo transitions by tunneling quantum-mechanically between the wells.

A fast fluctuator or TLS interacting with conduction electrons is usually described by the *non-magnetic* or *orbital Kondo model*, studied in great detail by Zawadowski and coworkers [23, 24] (it is defined and reviewed in more detail in Appendices B and C of paper II; for other reviews, see [39, 43, 44]):

$$H = H_{TSS} + \sum_{\vec{k}} \varepsilon_{\vec{k}} c^\dagger_{\vec{k}\sigma} c_{\vec{k}'\sigma} + \sum_{\vec{k}\vec{k}'} c^\dagger_{\vec{k}\sigma} [\, V^0_{\vec{k}\vec{k}'} + V^x_{\vec{k}\vec{k}'} \tau^x + V^z_{\vec{k}\vec{k}'} \tau^z \,] c_{\vec{k}'\sigma}. \tag{8}$$

Here $c^\dagger_{\vec{k}\sigma}$ creates an electron with momentum $\vec{k}$ and Pauli spin σ. The terms V^o and $V^z\tau^z$ describe *diagonal* scattering events in which the TLS-atoms do not tunnel between wells. The term $V^x\tau^x$ describes so-called *electron-assisted tunneling* processes. During these, electron scattering does lead to tunneling, and hence the associated bare matrix elements are much smaller than for diagonal scattering: $V^x/V^z \simeq 10^{-3}$.

Zawadowski and coworkers showed that the electron-assisted term $V^x\tau^x$ renormalizes to substantially larger values as the temperature is lowered (as does a

similar $V^y\tau^y$ term that is generated under renormalization). At sufficiently low temperatures (where $V^z \simeq V^x \simeq V^y$), the non-magnetic Kondo model was shown [45] to be equivalent to the standard 2-channel Kondo (2CK) model, with an effective interaction of the form

$$H_{int}^{eff} = v_K \int d\varepsilon \int d\varepsilon' \sum_{\alpha,\,\alpha'} \sum_{\sigma\sigma'} c^\dagger_{\varepsilon\alpha\sigma} (\tfrac{1}{2}\vec{\sigma}_{\alpha\alpha'} \cdot \tfrac{1}{2}\vec{\tau}) c_{\varepsilon\alpha'\sigma}. \tag{9}$$

The two positions of the fast fluctuator in the L- and R wells correspond to the spin up and down of a magnetic impurity (and L-R transitions to impurity spin flips). The electrons are labelled by an energy index ε, a so-called pseudo-spin index $\alpha = 1, 2$ (corresponding to those two combination of angular momentum states about the impurity that couple most strongly to the TLS), and the Pauli spin index $\sigma = \uparrow, \downarrow$. Evidently, α plays the role of the electron's magnetic spin index in the magnetic 2CK model, and since the effective interaction is diagonal in σ (which has two values), σ is the channel index.

This (non-magnetic) 2CK model, with strong analogies to the magnetic one, yields an electron scattering rate $\tau^{-1}(\varepsilon, T)$ with the properties [24, 46]

$$\tau^{-1}(\varepsilon, T) - \tau^{-1}(0, T) \propto \begin{cases} \ln[\max(T, \varepsilon)] & \text{if} \quad T > T_K, \\ T^{1/2}\tilde{\Gamma}(\varepsilon/T) & \text{if} \quad \Delta^2/T_K < T \ll T_K. \end{cases} \tag{10}$$

(The condition $\Delta^2/T_K < T$ is explained in Section VI.C.) Hence, for $T > T_K$ or $\Delta^2/T_K < T \ll T_K$, it yields [via Eq. (5)] a contribution to the conductance of $\delta\sigma(T) \propto \ln T$ or $T^{1/2}$, respectively. The latter is typical for the complicated non-Fermi-liquid physics characteristic of the 2CK model in the $T \ll T_K$ regime. In this respect the non-magnetic 2CK model differs in an important way from the (1-channel) magnetic Kondo model, for which the low-T scaling is of the Fermi liquid form ($\propto T^2$).

B. *Successes of the 2CK Interpolation*

We now turn to an interpretation of facts (Cu.1) to (Cu.9) in terms of the 2CK scenario [1, 2]. Our aim here is to sketch the physical picture underlying the scenario. Those aspects that require detailed analysis, such as the scaling behavior (Cu.6) and magnetic field dependence (Cu.8), will be discussed more fully in subsequent sections.

Qualitative features. The cooling and annealing properties (Cu.1) and (Cu.3) suggest that the ZBAs are due to *structural* defects or disorder that can anneal away at high temperatures [although the well-resolved phonon spectrum implies that only a small amount of such disorder can be present (Cu.5)]. This conclusion is reinforced by the remarkably complex and non-monotonic behavior of the ZBA under thermal cycling (Cu.3c), which indicates that the ZBA probes the detailed

configuration of individual defects, not just the average behavior of the entire constriction region. Subsequent experiments with Ti constrictions have shown that the structural disorder is located in the "bulk" of the bowl-shaped hole, not on its surface, and that it is caused by geometry-induced stress occuring in the metal in the bowl-shaped part of the constriction [see (Ti.1d), Section VII.A].

By assuming that the ZBA is due to fast TLSs, i.e. a specific type of structural defect, the 2CK scenario accounts for all of the properties mentioned in the previous paragraph. Property (Cu.4a), the disappearance of the ZBA upon the addition of 1% Au atoms, can then be attributed to the TLSs being pinned by the additional static impurities.

Logarithms and scaling. Next, we assume that the TLS-electron interaction is governed by Zawadowski's non-magnetic Kondo model, which renormalizes to the 2CK model at low energy scales. This explains a number of further facts. Firstly, the non-magnetic nature of the interaction explains the absence of a Zeeman splitting in a magnetic field (Cu.8b). Furthermore, the fact that the 2CK scattering rate $\tau^{-1}(\varepsilon, T)$ has a logarithmic form for $\varepsilon > T_K (> T)$ or $T > T_K (> \varepsilon)$ [see Eq. (10)] accounts, via Eq. (5), for the asymptotic logarithmic V- and T dependence (Cu.7) of $G(V, T)$ for $V > V_K (> T)$ or $T > T_K (> V)$. Thus, we identify the experimental crossover temperature T_K ($\simeq 3$ to 5 K) of (Cu.6a) with the Kondo temperature of the 2CK model.

Similarly, the scaling form of $\tau^{-1}(\varepsilon, T)$ for $\varepsilon, T \ll T_K$ [see Eq. (10)] accounts, via Eq. (5), for the observed scaling behavior (Cu.6) of $G(V, T)$ for $V < V_K$ and $T < T_K$. To be more particular, the very occurence of scaling behavior (Cu.6a), and the fact that the experimental scaling curve $\Gamma(v)$ of (Cu.6c) is universal, can be explained (see Section VI.A) by assuming that the system is in the neighborhood of some fixed point. Assuming this to be the 2CK non-Fermi-liquid fixed point, the experimentally observed scaling regime can be associated with the theoretical expected scaling regime of $\Delta^2/T_K < T < T_K$ and $V < T_K$. Moreover, the non-Fermi-liquid value of $\alpha = \frac{1}{2}$ that is then expected for the scaling exponent (see Section VI.A) agrees precisely with the value observed for α. Thus, within the 2CK interpretation, the experimental demonstration of $\alpha = \frac{1}{2}$ is equivalent to the direct observation of non-Fermi-liquid behavior. Finally, it will be shown in paper II that the shape of the universal scaling curve $\Gamma(v)$ is also in quantitative agreement with the 2CK model.

Number of TLSs. Each 2CK impurity in the constriction can change the conductance by at most $2e^2/h$.[2] Therefore, the sample with the largest ZBA of $70e^2/h$ (sample #2 in Fig. 7) would require up to about 40 such TLSs in the constriction. However, this is still only a relatively small amount of disorder

[2] To see this, we note that in the unitary limit the scattering rate of electrons off a k-channel Kondo defect is proportional to $k \sin^2 \delta$ (see e.g. [47, Eq. (2.20)]), and the phase shift at the intermediate-coupling fixed point is $\delta = \pi/2k$ [48]. Thus, in the unitarity limit, the contribution to the resistance of a $k = 2$ Kondo impurity is the same as for $k = 1$, namely $2e^2/h$ (the 2 comes from Pauli spin).

(corresponding to a density of about 10^{-4} TLSs per atom [11, p. 277][3]). The sample that showed the best scaling (sample #1 in Fig. 5) had a significantly smaller amplitude of $\lesssim 20e^2/h$, implying only about 10 active TLSs (that samples with a smaller amplitude should show better scaling is to be expected due to a smaller spread in Δ's, see (Ti.3) in Section VII.A).

C. *Open Questions in the 2CK Scenario*

Having discussed the successes of the 2CK scenario, we now turn to questions for which the 2CK scenario is unable to offer a detailed explanation, namely the conductance transitions (Cu.9), the strong magnetic field dependence (Cu.8a), and the microscopic nature of the TLSs. We shall point out below that (Cu.9) and (Cu.8a) are not generic to TLS-induced ZBAs, and speculate that they are related and must involve some new "high-energy" physics, since (Cu.9) occurs at a large voltage V_c. Therefore, our lack of understanding of the latter need not affect the 2CK interpretation of the low-energy scaling behavior (Cu.6). We conclude with some speculations about the microscopic nature of the TLSs, and the likelihood that realistic TLSs will have all the properties required by the 2CK scenario.

1. *Conductance Transitions*

The fact that conductance transitions occur only in samples that have a ZBA (Cu.9a) suggests [32] that these are related to the ZBA: if the latter is phenomenologically viewed as the manifestation of some strongly correlated state of the system, then conductance transitions correspond to the sharp, sudden, "switching off" of the correlations as V becomes too large. For example, in the 2CK interpretation, interactions of electrons with TLSs in the constriction give rise to a strongly correlated non-Fermi-liquid state at small T and V. One might speculate that if for some reason a large voltage could "freeze" the TLSs, i.e. prevent them from tunneling, this would disrupt the correlations and give rise to a sudden change in the DC conductance and hence a spike in the differential conductance.

At present we are not aware of any detailed microscopic explanation for the conductance transitions. Note, though, that they do not occur in *all* Cu samples showing ZBAs. Moreover, recent experiments by Upadhyay *et al.* [19] on Titanium constrictions and by Keijsers *et al.* [20] on constrictions made from metallic glasses showed TLS-induced ZBAs with properties very similar to RB's quenched Cu constrictions, but no conductance transitions at all (see (Ti.6) and (MG.4) in

[3] For Example, the 6.4 Ω constriction studied in [1] has a diameter of ~ 13 nm [estimated via the Sharvin formula Eq. (3)], and there are 10^5 Cu atoms within a sphere of this diameter about the constriction. Assuming on the order of ~ 40 active TLSs, their density is therefore roughly of order 10^{-4}/atom. Although the constriction is believed to be crystalline, not glassy, it is worth noting that this density of TLSs is about the same as estimates for the total density of TLSs in glassy systems.

Section VII, where these experiments are reviewed). This suggests that *conductance transitions are not a generic ingredient of the phenomenology of ZBAs induced by TLSs*. Moreover, in the quenched Cu samples, provided that H and T are sufficiently small, the transition voltage V_c at which the first conductance transition occurs usually lies well above T_K, the scale characterizing the extent of the low-energy scaling regime of the ZBA [see Fig. 2(a)]. (In other words, since they don't occur near zero bias, the conductance transitions need not be viewed as part of the zero-bias anomaly phenomenon at all, if one restricts this term to refer only to the low-energy regime.)

Thus, there seems to be a clear separation of energy scales governing the ZBA and the conductance transitions. The latter must therefore be governed by some new large energy scale due to a mechanism not yet understood. However, due to the separation of energy scales, the conductance transitions need not affect our description of the low-energy scaling regime of the ZBA below T_K (which is $\ll eV_c/k_B$) in terms of the 2CK model.

2. *Strong Magnetic Field Dependence*

Since the electron-TLS interaction is non-magnetic, i.e. not directly affected by a magnetic field, the 2CK scenario predicts no, or at best a very weak magnetic field dependence for the ZBA. This agrees with the absence of a Zeeman splitting of the ZBA for the Cu samples (Cu.8b) (which was in fact one of the main reasons for the proposal of the non-magnetic 2CK interpretation [1]). However, it leaves the strong magnetic field dependence (Cu.8a) as a puzzle. (Two indirect mechanism for H to couple to a 2CK system, namely via H-tuning of the asymmetry energy $\Delta_z(H)$ and via channel symmetry breaking, are investigated in Appendix B; they are found to be too weak to account for (Cu.8a), contrary to the interpretation we had previously offered [2].)

It is therefore very significant that the experiments by Upadhyay *et al.* on Ti constrictions and by Keijsers *et al.* on metallic-glass constrictions show ZBAs with only a very weak or even no H-dependence [see Section VII, (Ti.5), (MG.3)], in complete accord with 2CK expectations. This suggests that, just as the conductance transitions, *the strong magnetic field dependence* (Cu.8a) *of the quenched Cu constrictions is not a generic feature of TLS-induced ZBAs*. Moreover, Fig. 13 suggests that in the Cu samples these two properties might be *linked*, because it shows that the strong H-dependence of $G(V=0, H)$ is related to the fact that the transition voltage V_c decreases to 0 as H is increased (Cu.9b,v). (In other words, if the strongly correlated state sets in at smaller V_c as V is lowered, the voltage-regime $0 < V < V_c$ in which the anomaly can develop is smaller, so that its total amplitude is smaller.)

Since the main difference between the Cu constrictions and the Ti and metallic-glass constrictions seems to be that the former contain TLSs with very small Δ's (see the next subsection), whereas in the latter, being disordered materials, there will certainly be a broad distribution of splittings, we speculate that the conductance

spikes and strong H-dependence might both be a consequence of the very small Δs occuring in the Cu samples, perhaps due to interactions between several TLSs with very small splittings.

Thus, we conclude that attempts (such as those in [2]) to explain the H-dependence of the ZBA (even at $V=0$) purely in terms of the 2CK model, which captures only the physics at low energies below T_K, are misdirected, because the H-dependence would arise, via the conductance transitions, from the "high-energy" physics associated with the large scale V_c.

This interpretation, according to which a magnetic field does not directly affect the low-energy physics of the phenomenon (only indirectly via its effect on V_c), can be checked by doing a V/T scaling analysis at fixed but small, non-zero magnetic field. If H is sufficiently small that the conductance transitions still occur at relatively high voltages (i.e. $V_c > T_K$), the scaling properties of (Cu.6) should not be affected by having $H \neq 0$). The presently available data is unfortunately insufficient to test this prediction.

The conclusions of this and the previous subsection are summarized in assumptions (A3) and (A4) in subsection V.D.

3. *Microscopic Nature of the TLS*

Finally, the 2CK interpretation is of course unable to answer the question: What is the microscopic nature of the presumed TLSs? Now, ignorance of microscopic details does not affect our explanation for why the scaling properties (Cu.6) of the ZBA seem to be universal: because the latter are presumably governed by the *fixed point* of the 2CK model, any system that is somewhere in the vicinity of this fixed point will flow towards it as the temperature is lowered (provided that relevant perturbations are sufficiently small) and hence exhibit the same universal behavior, irrespective of its detailed bare parameters.

However, the quality of the scaling behavior implies some rather stringent restrictions on the allowed properties of the presumed TLSs, because we need to assume that all active TLSs (e.g. about 10 for sample #1, which shows the best scaling) are close enough in parameter space to the non-Fermi-liquid fixed point to show pure scaling.

This implies, firstly, that interactions between TLSs (which are known to exist in general [34], mediated by strain fields and changes in electron density), must be negligible, because they would drive the system away from the 2CK non-Fermi-liquid fixed point. Secondly, the fact that scaling is only expected in the regime $\Delta^2/T_K < T < T_K$ can be used to estimate that $T_K \simeq 3$ to 5K and $\Delta \lesssim 1$ K (see Section VI for details). Kondo temperatures in the range of 1–10 K are in good agreement with the most recent theoretical estimates for TLSs [49]. However, the condition $\Delta \lesssim 1$ K implies that for active TLSs the distribution of energy splittings, $P(\Delta)$, must be peaked below $\Delta \lesssim 1$ K. Since $\Delta = (\Delta_z^2 + \Delta_x)^{1/2}$, both the asymmetry energy Δ_z and tunneling rate Δ_x must be $\lesssim 1$ K, a value so small that it needs further comment.

First note that it is not immediately obvious that values of the bare tunneling rate Δ_x exist at all that allow 2CK physics: For transitions to be able to take place, the barrier between the wells must be sufficiently small, but a small barrier is usually associated with a large bare Δ_x, implying a large bare Δ (and Δ sets the energy scale at which the renormalization flow toward the non-Fermi-liquid fixed point is cut off). Now, for a TLS in a metal, the physics of screening can reduce the direct tunneling rate Δ_x by as much as three orders of magnitude under renormalization to $T \ll T_K$ [50] (when tunneling between the wells, the tunneling center has to drag along its screening clowd, which becomes increasingly difficult, due to the orthogonality catastrophy, at lower temperatures). Thus, the renormalized direct tunneling rate can always be assumed very small. Though this implies a large effective barrier, it does not necessarily prohibit 2CK physics: Zaránd and Zawadowski [49, 51] have shown 2CK physics can be obtained even if $\Delta_x = 0$, provided that the model contains some other channel for inter-well transitions, such as electron-assisted transitions via more highly excited TLS states (see Appendix C.5 of II).

More serious is the assumption that the renormalized asymmetry energy Δ_r also be $\lesssim 1$ K. This may seem very small when recalling that in glassy materials, the distribution $P(\Delta)$ for the asymmetry energy is rather flat, with Δ varying over many (often tens of) Kelvins. Note, though, that far from being glassy, the constrictions are believed to be rather clean (Cu.5), containing almost perfectly crystalline Cu. Therefore, our intuition about the properties of TLSs in glasses can not be applied to the present system. For example, the TLSs could possibly be dislocation kinks. (This would naturally account for the disappearance of the ZBA when static disorder is added (Cu.4a), since dislocation kinks can be pinned by other defects.) Since the dislocation kink would find itself in a rather crystalline material, some lattice symmetry could guarantee then that the two wells of the TLS are (nearly) degenerate and hence assure a small Δ_z and hence small Δ, etc.

Moreover, some role might be played by the mechanism of "autoselection": This assumes that a given TLS will only be "active", in the sense of contributing to the non-trivial V- and T-dependence of the conductance, if its (renormalized) parameters happen to be in the appropriate non-Fermi-liquid regime; if they are not, the TLS would only be an "inactive spectator" that only affects the V- and T-*independent* background conductance G_o. Moreover, provided that the distribution $P(\Delta_z)$ is not zero near $\Delta_z = 0$ (which seems very unlikely), there should always exist a few TLSs with $\Delta \lesssim 1$ K, since Δ_x is strongly reduced by screening.

Despite the above arguments, the fact that the effects of non-zero Δs did not show up in the quenched Cu samples, necessitating the assumption that all active TLSs must have $\Delta \lesssim 1$ K, remains probably the weakest point the 2CK interpretation of these samples. Therefore it is very significant that the effects of non-zero Δs were recently explicitly demonstrated in the Ti constrictions of Upadhyay *et al.*: in some samples scaling *breaks down* below an energy scale associated with Δ, which was found to be tunable by electromigration and the application of a magnetic field [see Section VII.A, (Ti.4), (Ti.5)]. Thus, the new Ti experiments significantly bolster the 2CK scenario at its hitherto weakest point.

To shed further light on the effects of non-zero Δ, it would be interesting if ZBA experiments with *specific* type of defects with *known* parameters could be performed.

It should be mentioned that Wingreen, Altshuler and Meir (WAM) have recently claimed [15](a) that the 2CK interpretation is internally inconsistent if one takes into account the effect of static disorder: using values for the coupling constants deduced from the observed Kondo temperatures, they concluded that renormalized energy splitting Δ would be dramatically increased (to typical values of about 100K), and in particular that there would be zero probability for zero splitting ($P(0)=0$). However, since their arguments neglected the physics of screening (i.e. the strong reduction of Δ_x under renormalization to lower temperatures), we believe that their conclusions, in particular that $P(0)=0$, are not persuasive [15](b), [50]. A critical discussion of their arguments is given in Appendix D of paper II.

D. *Summary of Assumptions of 2CK Scenario*

The 2CK interpretation of the ZBA in quenched Cu constrictions developed in this section can be summarized in the following assumptions:

(A1) The ZBA is due to the presence in the constriction region of structural defects, namely TLSs, that interact with conduction electrons according to the non-magnetic Kondo model, which renormalizes at low energies to the non-Fermi-liquid regime of the 2CK model.

(A2) The TLSs may occur with a distribution of (dressed or renormalized) parameters, but all "active" TLSs, i.e. those which contribute measurably to the voltage dependence of the conductance in the Cu point contacts, must have parameters which cause their behaviors to be governed by the physics of the non-Fermi-liquid fixed point of the 2CK model. This requires that all of these active TLSs do not interact with each other. Moreover, pure V/T scaling will only occur in the window $\Delta^2/T_K < T < T_K$ (in quenched Cu samples it was found for $T > 0.4$ K and $T_K > 3$ to 5 K, implying $\Delta \lesssim 1$ K). Note though, that the absence of *scaling* for $T < \Delta^2/T_K$ does not necessarily imply the absence of non-Fermi-liquid physics, which can still show up as $V^{1/2}$ behavior for $\Delta^2/T_K < V < T_K$.

(A3) The large magnetic field dependence (Cu.8a) and the conductance transitions (Cu.9) of the quenched Cu ZBAs are related, but not generic to the ZBA. They cannot be explained by 2CK physics alone, but involve some new energy scale on the order of V_c.

(A4) A magnetic field does not *directly* influence the low-energy physics ($V < V_K$, $T < T_K$) of the ZBA. Therefore, 2CK physics can account for the behavior of the ZBA in quenched Cu samples at fixed H, provided that H is sufficiently small ($\lesssim 1$ T) that the conductance transitions do not influence the 2CK scaling regime (i.e. $V_c > V_K$).

VI. SCALING ANALYSIS OF $G(V, T)$

In this section, we present a detailed scaling analysis of the data and establish the scaling properties of (Cu.6). This is a very important part of the analysis of the experiment, since the scaling properties were used above to eliminate quite a number of otherwise plausible candidate explanations of the ZBA. Nevertheless, since the upshot of this section is contained completely in property (Cu.6), this section can by skipped by readers not interested in the details of the scaling analysis.

Of course, the scaling properties (Cu.6) we are about to establish are simply experimental facts, independent of any theoretical interpretation. Nevertheless, during the writing of Ref. [2], these properties were predicted (before their experimental verification) on the basis of the CFT solution of the 2CK model, and we shall present our analysis within this framework. We begin by giving in Section VI.A the general scaling argument first reported in [2] to motivate the scaling Ansatz for the conductance $G(V, T)$, and a back-of-the-envelope calculation of the scaling function $\Gamma(x)$. A more careful calculation, tailored to the nanoconstriction geometry and its non-equilibrium peculiarities, is reserved for paper II.

A. *The Scaling Ansatz*

The 2CK model is known [9] to flow to a non-trivial, non-Fermi-liquid fixed point at $T=0$, at which the model has been solved exactly by Affleck and Ludwig (AL), using CFT [10]. This fixed point governs the physics in the non-Fermi-liquid regime, namely $\Delta^2/T_K < T < T_K$ and $V < V_K$. We shall now show by a general scaling argument [2] that the assumption of proximity to this fixed point (A2), implies the scaling properties (Cu.6) of the conductance $G(V, T)$.

1. *General Scaling Argument*

Consider first the conductance signal $G_i(V, T)$ due to a single TLS (labeled by the index i) with $T \ll T_K^i$, $eV \ll k_B T_K^i$, $\Delta_i = 0$, but *arbitrary* ratio $eV/k_B T$. According to the general theory of critical phenomena, one expects that physical quantities will obey scaling relations in the neighborhood of any fixed point. For the conductance in the present case, a natural scaling Ansatz is

$$G_i(V, T) = G_{io} + B_i T^{\alpha}\, \Gamma\left(\frac{A_i eV}{(k_B T)^{\alpha/\beta}}\right). \tag{11}$$

The parameters A_i and B_i are non-universal, positive constants, analogous to the $a_i^{\pm}$ and b_i of Eq. (4), which may vary, for instance, as a function of the position of the TLSs within the constriction. However, the function $\Gamma(v)$ should be a *universal function*, a fingerprint of the 2CK model that is the same for *any* microscopic realization thereof. It must have the asymptotic form $\Gamma(v) \propto v^{\beta}$ as $v \to \infty$, since

$G(V, T)$ must be independent of T for $eV \gg k_B T$. Due to the arbitrariness of A_i and B_i, we are free to use the normalization conventions that

$$\Gamma(0) \equiv 1, \qquad \Gamma(v) = v^\beta + \text{constant} \qquad \text{as} \quad v^\beta \to \infty. \tag{12}$$

Now, *if V is small enough*, its only effect will be to create a slightly non-equilibrium electron distribution in the leads. In particular, effects that directly affect the impurity itself, like V-dependent strains, or the "polarization" of the TLS in one well due to the non-equilibrium electron distribution, etc. can then be neglected. In this case, which we shall call the *weakly non-equilibrium regime*, V only enters in the Fermi functions of the leads, in the form $[\, e^{\beta(\varepsilon - eV/2)} + 1\,]^{-1}$, i.e. in the combination $eV/k_B T$, implying $\alpha = \beta$.

For a constriction with several defects, the conductance signal will be additive,[4] i.e. (now using $\alpha = \beta$):

$$G(V, T) = G_o + T^\alpha \sum_i B_i \Gamma\left(\frac{A_i eV}{k_B T}\right). \tag{13}$$

Subtracting $G(0, T)$ from this to eliminate G_o then immediately results in the scaling relation of (Cu.6a):

$$\frac{G(V, T) - G(0, T)}{T^\alpha} = \sum_i B_i [\, \Gamma(A_i v) - 1\,] \equiv F(v)\,. \tag{14}$$

The scaling function $F(v)$ defined on the right-hand side is non-universal, since it depends on the A_i and B_i.

This is as far as general scaling arguments will take us; a specific theory is needed to predict α. To this end, we argue by analogy with the conductivity of a *bulk* metal containing 2CK impurities. There the bulk conductivity $\sigma(T)$ is determined, via the Kubo formula,

$$\sigma(T) = 2\,\frac{e^2}{3m^2} \int \frac{d^3p}{(2\pi)^3}\, [\, -\partial_{\varepsilon_p} f_o(\varepsilon)\,]\, \vec{p}^{\,2} \tau(\varepsilon_p), \tag{15}$$

by the elastic scattering life-time $\tau^{-1}(\varepsilon) = -2\,\mathrm{Im}\,\Sigma^R(\varepsilon)$, where $\varepsilon \equiv \varepsilon_p - \varepsilon_F$, and $\Sigma^R(\varepsilon)$ is the retarded electron self-energy. $\Sigma^R(\varepsilon)$ has been calculated exactly by Affleck and Ludwig, using CFT [46], for the bulk k-channel Kondo problem in the neighborhood of its $T = 0$ fixed point (i.e. for $T \ll T_K$). They found that in general τ^{-1} has the following scaling form (motivated in paper III, or [46], [14, Chapter 8]):

$$\tau^{-1}(\varepsilon, \{\lambda_m\}) \equiv -2\,\mathrm{Im}\,\Sigma^R(\varepsilon, \{\lambda_m\}) = \tau_o^{-1} \left[\, 1 + \sum_m \lambda_m T^{\alpha_m} \tilde{\Gamma}_m(\varepsilon/T) \right]. \tag{16}$$

[4] To be more precise: the contributions of the impurities to the resistance $R = G^{-1}$ are additive, but since $R = R_o + \sum_i \delta R_i(V, T)$, with $R_o \gg \delta R_i(V, T)$, the form (13) follows.

The sum on m is over all perturbations to the fixed point action that one wants to consider. Each such perturbation is characterized by a non-universal parameter λ_m which measures its strength (and has dimensions of $E_m^{-\alpha_m}$, where E_m is the energy scale characterizing this perturbation), a universal scaling dimension α_m and a (dimensionless) universal scaling function $\tilde{\Gamma}_m(x)$. In principle all the α_m and $\tilde{\Gamma}_m(x)$ (but not the non-universal λ_m) can be calculated exactly from CFT, provided all the $\lambda_m T^{\alpha_m}$ are small enough that one is in the close vicinity of the fixed point. Perturbations with $\alpha_m < 0$ or > 0 are relevant or irrelevant, respectively, because they grow or decrease as the temperature is lowered at fixed λ_m. For all perturbations of interest in this paper, the scaling functions have the properties $\tilde{\Gamma}_m(x) = \tilde{\Gamma}_m(-x)$ and $\tilde{\Gamma}_m(x) \propto x^{\alpha_m}$ as $x \to \infty$ (the latter property follows because the perturbation must become T-independent in the limit $\varepsilon \gg T$).

AL have calculated in detail the *leading* irrelevant correction to τ_o^{-1} for the k-channel Kondo problem, for the case that no relevant perturbations are present. In other words they take $\lambda_m = 0$ for all m for which $\alpha_m < 0$, and consider only the correction corresponding to the smallest $\alpha_m > 0$, say α_1. When referring only to this correction, we shall drop the subscript $m = 1$ and denote the corresponding parameters by $\lambda_1 \equiv \lambda$, $\alpha_1 \equiv \alpha$ and $\tilde{\Gamma}_1(x) \equiv \tilde{\Gamma}(x)$. They showed that for the k-channel Kondo problem $\alpha = 2/(2+k)$, $\lambda = \tilde{\lambda} T_K^{-\alpha} > 0$ (where $\tilde{\lambda}$ is a dimensionless number of order unity) and $\tilde{\Gamma}(x) < 0$.[5] (For an explicit expression for $\tilde{\Gamma}(x)$, see [46, Eq. (3.50)] or paper II).

Considering only this leading irrelevant perturbation, it follows immediately from the Kubo formula that for the 2CK problem ($k = 2$, hence $\alpha = \frac{1}{2}$), the bulk conductivity has the form

$$\sigma(T) = \sigma_o + \left(\frac{T}{T_K}\right)^{1/2} \sigma_1, \tag{17}$$

with $\sigma_1 > 0$. The unusual power law $T^{1/2}$ is a signature of the non-Fermi-liquid nature of the $T = 0$ fixed point. For a Fermi liquid, one would have had T^2.

Although the form (19) for $\tau^{-1}(\varepsilon)$ was derived by AL only for a bulk geometry, it is natural to assume that it also governs the conductance in the nanoconstriction geometry (paper II is devoted to a careful justification of this assumption). This implies that the exponent in Eq. (11) should also be $\alpha = \frac{1}{2}$, which completes our general-principles motivation for the scaling Ansatz.

2. *Back-of-the-envelope calculation of $\Gamma(v)$*

If one is willing to gloss over important subtleties, it is possible to obtain by a simple back-of-the-envelope calculation a quantitative expression for the scaling function that agrees with that found by more careful means in paper II.

[5] The sign of λ is *a priori* undetermined in the CFT approach (see [46, after Eq. (3.64)]); however, to conform to the expectation that the Kondo scattering rate increases as ε or T are decreased, we need $\lambda > 0$, since $\tilde{\Gamma}(x) < 0$.

Our starting point is Eq. (4), which gives the change in conductance due to back-scattering off defects in a nanoconstriction in terms of the scattering rate $\tau^{-1}(\varepsilon)$. Now, the main difference between a bulk metal and a nanoconstriction is that the latter represents a decidedly non-equilibrium situation. However, in the *weakly* non-equilibrium regime, i.e. if the voltage is small enough ($V < V_K$), it is a reasonable guess (which is substantiated in II) that the form of the scattering rate of electrons off a TLS in the nanoconstriction is not all that different as when the TLSs are in the bulk. Hence, let us boldly use[6] the *equilibrium* form for τ^{-1}, namely Eq. (16), in Eq. (4) for ΔG, thus obtaining (to lowest order in λ_m)

$$G(V, T, \{\lambda_m\}) = G_o - e^2/h \sum_m \lambda_m T^{\alpha_m} \int d\varepsilon [-\partial_\varepsilon f_o(\varepsilon)] \times \sum_i b_i \tfrac{1}{2} [\tilde{\Gamma}_m(\varepsilon - \tfrac{1}{2} eV a_i^+) + \tilde{\Gamma}(\varepsilon + \tfrac{1}{2} eV a_i^-)]. \tag{18}$$

Now write $\varepsilon/k_B T \equiv x$, $eV/k_B T \equiv v$, $f_o(v) \equiv [e^v + 1]^{-1}$, and define (universal) functions $\Gamma_m(v)$ by

$$\gamma_{b,m} \Gamma_m(\gamma_{a,m} v) \equiv \int dx [\partial_x f_o(x)] \tilde{\Gamma}_m(x + v/2). \tag{19}$$

Here $\gamma_{a,m}$ and $\gamma_{b,m}$ are universal constants, chosen such that $\Gamma_m(v)$ is normalized as in Eq. (12), with $\Gamma_m(\infty) > 0$:

$$\Gamma_m(0) \equiv 1, \qquad \Gamma_m(v) = v^{\alpha_m} + \text{constant}, \qquad \text{as} \quad v^{\alpha_m} \to \infty. \tag{20}$$

Using the property $\tilde{\Gamma}_m(x) = \tilde{\Gamma}_m(-x)$ in the first term of Eq. (18), we find

$$G(V, T, \{\lambda_m\}) = G_o + e^2/h \sum_m \lambda_m T^{\alpha_m} \gamma_{b,m} \sum_i b_i \times \tfrac{1}{2} [\Gamma_m(a_i^+ \gamma_{a,m} v) + \Gamma_m(a_i^- \gamma_{a,m} v)]. \tag{21}$$

[6] The justification for this assumption is explained in Section V.2 of paper II; essentially, we assume that the leading non-equilibrium corrections to τ^{-1} are of order V/T_K, which are negligible in the weakly non-equilibrium or scaling regime.

Let us now specialize again to the leading irrelevant perturbation, for which only $\lambda_1 \equiv \lambda \neq 0$. (Since for this case $\tilde{\Gamma}(x) < 0$, $\gamma_{a,1} \equiv \gamma_a$ and $\gamma_{b,1} \equiv \gamma_b$ can both be chosen positive.) In this case, Eq. (21) is precisely of the form of the scaling Ansatz Eq. (13), with $\alpha = \frac{1}{2}$. Thus we have found a "derivation" for the scaling Ansatz.[7] Moreover, this little calculation has furnished us with an expression, namely Eq. (19), for the universal scaling function $\Gamma(v)$ in terms of the exactly known universal function $\tilde{\Gamma}(x)$.

This, in a nutshell, is all there is to the scaling prediction. Of course, to back up this result by a respectable calculation, considerably more care is required and several technical and conceptual hurdles have to be overcome. These are addressed in paper II. And finally, in paper III the origin of the exponent $\alpha = \frac{1}{2}$ is explained; AL originally derived it using the full machinery of CFT, but it in III it is found much more simply and directly using a recent reformulation [22] of their theory in terms of free boson fields.

B. *Scaling Analysis of Experimental Data*

In this section we summarize the results of a careful scaling analysis of the experimental data [2], based on Section 6.4.2 of [11], and establish that $G(V, T)$ has the properies summarized in (Cu.6) of Section IV.

1. *First Test of $T^{1/2}$ and $V^{1/2}$ Behavior*

As a first test of the scaling relation Eq. (13), one can consider it in the asymptotic limits $v \to 0$ and ∞, in which the conductance becomes [using Eq. (12)]

$$G(0, T) = G_o + T^{\alpha} B_{\Sigma}, \qquad \left(B_{\Sigma} \equiv \sum_i B_i \right); \tag{22}$$

$$G(V, T_o) = \text{const} + v^{\alpha} F_o \qquad \text{at fixed } T_o \ll eV/k_B \qquad \left(F_o \equiv \sum_i B_i A_i^{\alpha} \right). \tag{23}$$

Figs. 7(a) and 7(b) confirm that $G(0, T)$ and $G(V, 0)$ roughly conform to Eqs. (22) and (23), respectively, with $\alpha = \frac{1}{2}$. Values for B_{Σ} and F_o can be obtained from straight-line fits to these data, and are listed in Table I. However, the quality of these data is not good enough to rule out other values of α, ranging from 0.25 to 0.75.

[7] Note though that Eq. (11) is actually a little too simplistic, since in Eq. (21) each defect gives rise to two terms with different a_i^+ and a_i^-. Note also that b_i, γ_o are by definition all positive constants, and $\Gamma(x) > 0$. With the choice $\lambda > 0$, discussed in footnote 5, we therefore have $G(V, T, \lambda) - G(0, T, \lambda) > 0$, consistent with experiment.

2. *Scaling Collapse*

A much more stringent determination of α can be obtained from the scaling properties of the combined V and T dependence of the $G(V, T)$, which, according to the 2CK interpretation, should follow Eq. (14). To check whether the data obey this relation, the left-hand side of Eq. (14) should be plotted vs. v^{α}. Provided that the correct value of α has been chosen, the low-T curves for a given sample should all collapse, with no further adjustment of free parameters, onto the sample-specific scaling curve $F(v)$ vs. v^{α}, which should be linear for large v^{α} [by Eq. (23)]. By adjusting α to obtain the best possible collapse, α can be determined from the data rather accurately. The 2CK scenario predicts $\alpha = \frac{1}{2}$.

The raw data for the differential conductance $G(V, T)$ of sample #1 of Fig. 7 is shown in Fig. 8(a), for T ranging from 100 mK to 5.7 K. Using $\alpha = \frac{1}{2}$, rescaling as in Eq. (14) and plotting the left-hand side vs. $v^{1/2}$, these data have the form shown in Fig. 8(b). The data at low V and low T collapse remarkably well onto one curve, which we shall call the *scaling curve*. Furthermore, $F(v)$ vs. $v^{1/2}$ has linear asymptote as $v \to \infty$, in agreement with Eq. (23).

Most of the individual curves deviate from the scaling curve for V larger than a typical scale $eV_K \simeq 1$ meV (this is also roughly the voltage at which lower-lying curves in Fig. 8(a) begin to fall on top of each other). Likewise, the lowest curves in the figure, which correspond to the highest temperatures, deviate from the scaling curve for almost all V. These deviations from scaling at high V and T are expected, since if either $V > V_K$ or $T > T_K$, the scaling Ansatz is expected to break down. We estimate T_K as that T for which the rescaled data already deviate from the scaling curve at $eV/k_B T \leqslant 1$. This gives $T_K \geqslant 5$ K for the defects of sample 1, which are reasonable values, as discussed in Section V.C.3, and establishes the empirical relation $eV_K \simeq 2k_B T_K$.

A somewhat complimentary estimate for the highest Kondo temperatures of the TLSs in these samples comes from the temperature at which the zero-bias signals first become visible as the samples are cooled. For all 3 samples featured here, this value is approximately 10 K.

The quality of the scaling provides an exacting test of the exponent in the scaling Ansatz. Using $\alpha = 0.4$ or 0.6 instead of 0.5 in Eq. (14) produces a clear worsening of the collapse of the data (see Fig. 2(b) of [2]). As a quantitative measure of the quality of scaling, we define the parameter $D(\alpha)$, which is the mean square deviation from the average scaling curve $\bar{F}(v) \equiv (1/N) \sum_{n=1}^{N} F_n(v)$ (where n labels the different experimental curves, corresponding to different temperatures T_n), integrated over small values of $|v|$:

$$D(\alpha) \equiv \frac{1}{N} \sum_{n=1}^{N} \int_{-v_{max}}^{v_{max}} dv [F_n(v) - \bar{F}(v)]^2. \tag{24}$$

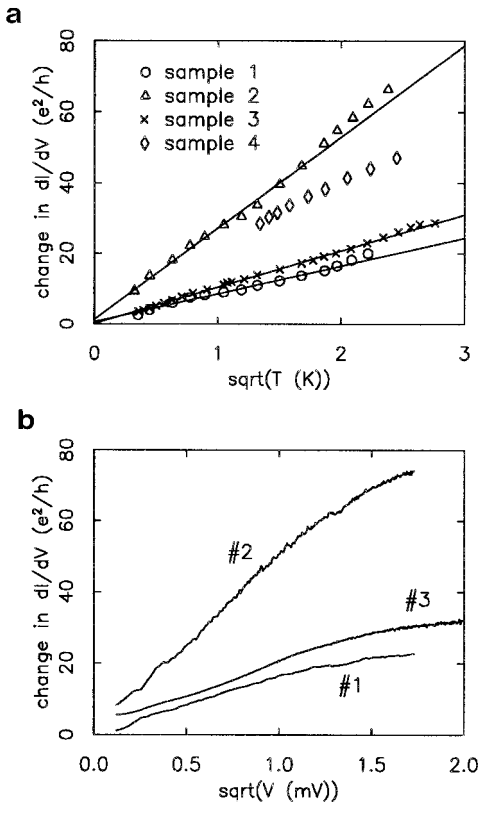

Fig. 7. (a) Temperature dependence of the $V=0$ conductance $[G(0,T)-G(0,T_o)]$ for the 4 unannealed Cu samples of Fig. 5, plotted versus $T^{1/2}$. The values of $G(0,T)$ for the different samples, exptrapolated to $T=0$ as shown are for sample #1: 2829 e^2/h, sample #2: 3973 e^2/h, sample #3: 30.8 e^2/h, and sample #4: approximately 2810 e^2/h. (b) Voltage dependence of the differential conductance at $T=100$ mK for some of the same samples as in (a), plotted versus $V^{1/2}$. The size of deviations from $T^{1/2}$ behavior in (a) (1 part in 3000) is consistent with the magnitude of amplifier drift in these measurements, as they were performed over several days. The V-dependent measurements in (b) are less subjective to such drift problems, as they are taken over a much shorter time span.

$D(\alpha)=0$ would signify perfect scaling. Taking the 5 lowest T ($\leqslant 1.4$ K) and $v_{max}=8$ (these are the data which *a priori* would be expected to be most accurately within the scaling regime, since they are closest to the $T=0$ fixed point), one obtains Fig. 9(a). Evidently the best scaling of the data requires $\alpha=0.48\pm0.05$ [the estimated uncertainty of ±0.05 comes from the uncertainty in the exact minimum in the curve in Fig. 9(a)]. This is in remarkably good agreement with the CFT prediction of $\alpha=\frac{1}{2}$.

We have also tested the more general scaling form of Eq. (11), and have observed scaling for $0.2<\alpha<0.8$, with $(\beta-0.5)\approx(\alpha-0.5)/2$, with best scaling for $\alpha=0.5\pm0.05$. But as argued earlier on page 20, one expects $\alpha=\beta$ on general grounds.

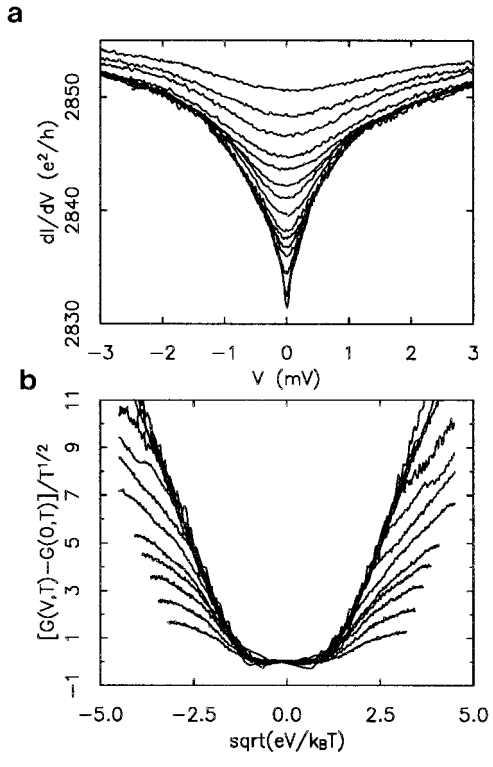

Fig. 8. (a) Voltage dependence of the differential conductance for sample #1 of Fig. 7, plotted for temperatures ranging from 100 mK (bottom curve) to 5.7 K (top curve). (b) The same data, rescaled according to Eq. (14) with $\alpha = \frac{1}{2}$, and plotted vs. $v^{1/2} = (eV/k_B T)^{1/2}$. The low-temperature, low-voltage data collapse onto a single curve [linear for large $v^{1/2}$, in agreement with Eq. (23)], with deviations when the voltage exceeds 1 mV.

The scaling Ansatz has also been tested on two other Cu samples. The rescaled data for sample 2 [Fig. 10(a)] collapse well onto a single curve at low V and T, for $\alpha = 0.52 \pm 0.05$ [Fig. 9(b)] and with $T_K \geqslant 3.5$ K. At high V and high T the non-universal conductance spikes of (Cu.9) are visible. The data for sample #3 do not seem to collapse as well [Fig. 10(b)] (illustrating how impressively accurate by comparison the scaling is for samples #1 and #2). However, we suggest that this sample in fact displays two separate sets of scaling curves (see arrows), one for $T \leqslant 0.4$ K and one for $0.6\ \text{K} \leqslant T \leqslant 5$ K, with interpolating curves in between. This could be due to defects with a distribution of T_K's, some having $T_K \simeq 0.4$ K and others having $T_K \geqslant 5$ K. The second (higher-T) set of curves do not collapse onto each other as well as the first, presumably because there is still some (approximately logarithmic) contribution from the $T_K \simeq 0.4$ K defects.

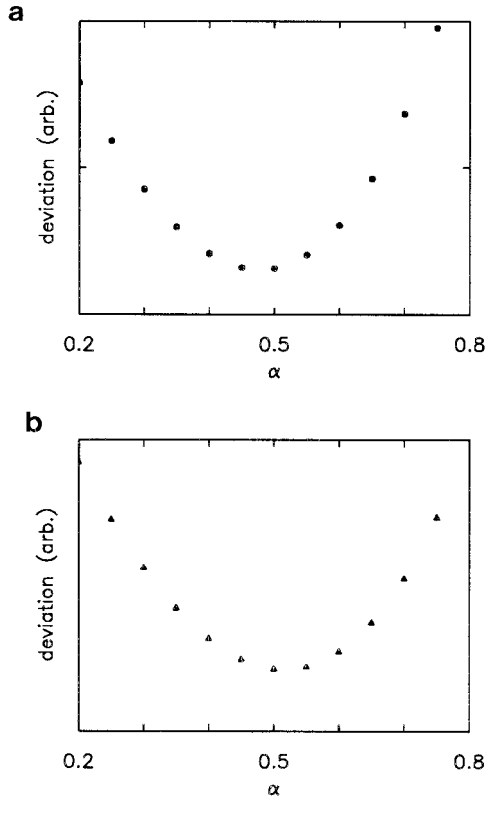

Fig. 9. The deviation parameter $D(\alpha)$ of Eq. (24), which quantifies the quality of scaling, for (a) sample #1 and (b) sample #2. The minimum of $D(\alpha)$ defines the value of α that gives the best scaling, giving $\alpha = 0.48 \pm 0.05$ for sample #1 and $\alpha = 0.52 \pm 0.05$ for sample #2.

3. *Universality*

If for any sample all the A_i in Eq. (14) were equal, one could directly extract the universal scaling curve from the data. The curve obtained by plotting

$$\frac{G(V, T) - G(0, T)}{B_\Sigma T^{1/2}} \qquad \text{versus} \qquad (AeV/k_B T)^{1/2}, \tag{25}$$

with A determined by the requirement that the asymptotic slope be equal to 1 [compare Eq. (12)], would be identical to the universal curve $(\Gamma(x) - 1)$ vs. $x^{1/2}$. Such plots are shown in Fig. 11(b). The fact that the scaling curves for all three samples are indistinguishable indicates that the distribution of A_i's in each sample is quite narrow and is a measure of the universality of the observed behavior.

To make possible quantitative comparisons of the data with the CFT prediction of Eq. (19), we now proceed to extract from the data the value of a universal

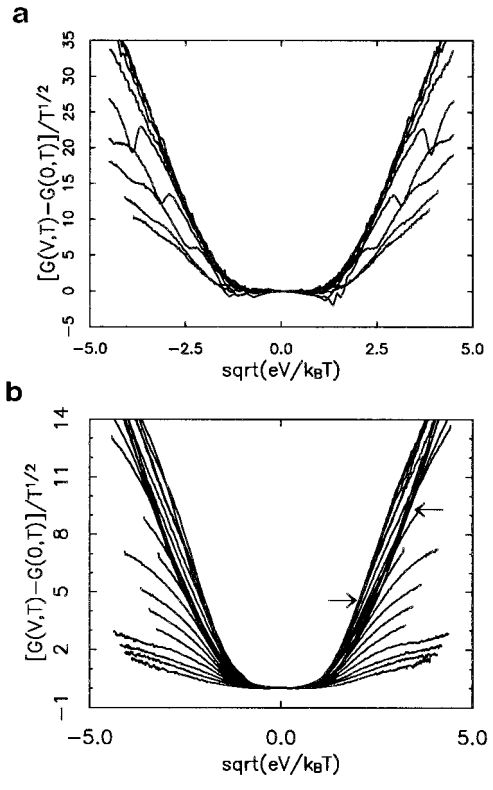

Fig. 10. (a) Differential conductance data for sample #2, at temperatures from 200 mK to 5.7 K, and (b) for sample #3, at temperatures from 50 mK to 7.6 K, rescaled according to Eq. (14) and plotted vs. $v^{1/2} = (eV/k_B T)^{1/2}$. The low-voltage, low-temperature data collapse well onto one curve for sample #2, but not for sample #3, partly due to the existence of TLSs with Kondo temperatures within (rather than above) the temperature range of the measurement.

(sample-independent) constant [essentially a Taylor coefficient of $\Gamma(v)$], which is independent of the possible distribution of A_i's and B_i's.

Consider the regime $v \gg 1$. As argued earlier, here $\Gamma(v) \simeq v^{\beta}$, and since $\beta = \alpha = 1/2$, with the normalization conventions of Eq. (12) we can write, asymptotically,

$$\Gamma(v) - 1 \equiv v^{1/2} + \Gamma_1 + O(v^{-1/2}), \tag{26}$$

where Γ_1 is a universal number. It characterizes how long the $\Gamma(v)$ curve stays "flat" for small v before bending upwards towards its asymtotic $v^{1/2}$-behavior. It follows from Eq. (14) that

$$F(v) = v^{1/2} F_0 + F_1 + O(v^{-1/2}), \tag{27}$$

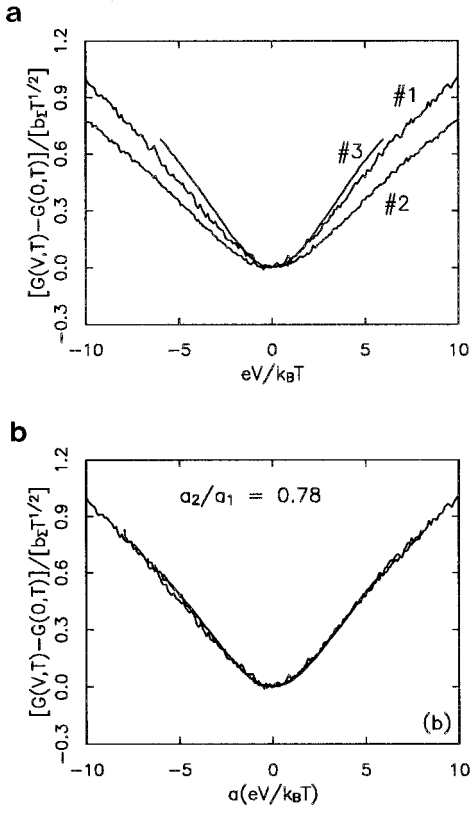

Fig. 11. Representatives conductance curves which lie along the scaling curves for samples #1, 2 and 3 of each of the three samples in Figs. 8(b), Fig. 10(a) and (b), respectively. For sample #1, the curve corresponds to T = 1.1 K, for sample #2 1.4 K, and for sample #3 250 mK. The reason for selecting these particular curves was that among all those lying along the scaling curve, they had the best signal-to-noise ratio for each sample. (a) The y-axis is scaled by the value of B_Σ determined from the temperature dependence of the $V=0$ conductance for each sample (values listed in Table 6.1). (b) In addition, the x-axis is scaled with a number a_i for each sample. The scaling curves for all three samples seem to lie on one universal curve.

where $F_0 \equiv \sum_i B_i A_i^{1/2}$ and $F_1 \equiv \Gamma_1 B_\Sigma$. Values for F_0 and F_1 may be determined from the conductance data by plotting F versus $v^{1/2}$ and fitting the data for large $v^{1/2}$ to a straight line. For samples 1 and 2 we fit between $(eV/k_BT)^{1/2} =$ 2 and 3, and for sample 3 (using only the curves below 250 mK) between 2 and 2.5.

Values for F_0, and F_1 are listed in Table I. The uncertainties listed are standard deviations of values determined at different T within the scaling regime for each sample. From these quantities, an experimental determination of the universal number $\Gamma_1 = F_1/B_\Sigma$ can be obtained; it is listed in Table I. The values of Γ_1 are consistent

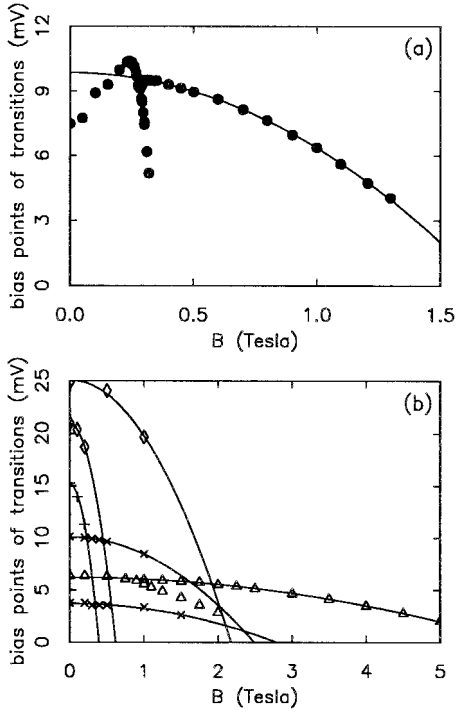

Fig. 12. (a) Transition voltage $V_c(H)$ of the conductance transition [32] as a function of magnetic field for a quenched Cu constriction at 4.2 K, showing bifurcation (Cu.9b, iv). At high fields $V_c(H) \to 0$ (Cu.9b, v), the dependence on H being quadratic. (b) $V_c(H)$ for five other samples at 4.2 K, with associated decreases to 0, quadratically in H.

among all 3 samples, in agreement with our expectation that Γ_1 should be a universal number.

Paper II will be devoted to a calculation of the universal scaling curve $\Gamma(v)$ and the universal number Γ_1. There it is shown that the quantitative predictions of the 2CK scenario are indeed consistent with the measured scaling curve.

TABLE I

Measured Parameters of the Scaling Functions for the ZBAs in 3 Cu Constrictions (Samples 1 to 3) and One Ti Constriction (Sample 4).

#	B_Σ	F_0	F_1	$\Gamma_1 = F_1/B_\Sigma$
1	7.8 ± 0.2	4.2 ± 0.3	-5.7 ± 0.9	-0.73 ± 0.11
2	25.2 ± 0.7	12.8 ± 0.8	-19.7 ± 1.5	-0.78 ± 0.06
3	10.3 ± 0.4	6.0 ± 0.6	-7.7 ± 1.6	-0.75 ± 0.16
4	1.69 ± 0.2	0.89 ± 0.05	-1.37 ± 0.1	-0.81 ± 0.10

Note. B_Σ, F_o and F_1 have units $K^{-1}e^2/h$, and Γ_1 is dimensionless.

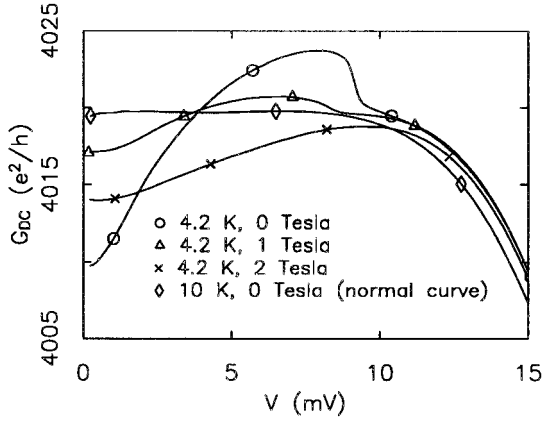

Fig. 13. The *DC* conductance G_{DC} (as opposed to differential conductance G used in all other plots) at several magnetic fields for a quenched Cu sample [32]. An increasing magnetic field broadens the conductance transition at V_c and moves V_c toward zero voltage, destroying the enhancement at $V = V_c$ of G_{DC} above the normal conductance. Note that although a large applied magnetic field eliminates the conductance transition, a $V = 0$ minimum in the conductance remains.

C. *Upper Bound on the Energy Splitting* Δ

The energy splitting Δ of a TLS is a relevant perturbation to the degenerate 2CK fixed point. In the language of the magnetic Kondo problem, it acts like a local magnetic field, and hence has scaling dimension $-\frac{1}{2}$ (see (3.19) of [52], or [39, Section 3.4.1 (e)]). Therefore a non-zero Δ implies that the electron scattering rate $\tau^{-1}(\varepsilon)$ and hence the conductance $G(V, T)$ will contain correction terms (to be labelled by $m = 2$), given by Eqs. (16) and (21), respectively, with $\alpha_2 = -\frac{1}{2}$ and $\lambda_2 = \tilde{\lambda}_2 \Delta / E_2^{1/2}$. Here $\tilde{\lambda}_2$ is a dimensionless number of order unity, and E_2 is an energy that sets the scale at which Δ becomes important. Though this scale is not *a priori* known in AL's CFT treatment, we shall take $E_2 = T_K$, since no other obvious energy scale suggests itself.

It follows that such Δ-dependent corrections, which would spoil good V/T scaling, are unimportant only if $\lambda_2 T^{\alpha_2} < 1$, i.e. as long as

$$\Delta < (T T_K)^{1/2} \tag{28}$$

holds for each active TLS. Note that this inequality allows Δ to be somewhat larger than the naive estimate that would follow from $\Delta < T$. As emphasized by Zawadowski [53], this somewhat enlarges the window of parameter space in which the 2CK scenario is applicable.

The above analysis enables us to estimate an upper bound on the energy splittings of active TLSs occuring in the quenched Cu samples. The data for samples 1 and

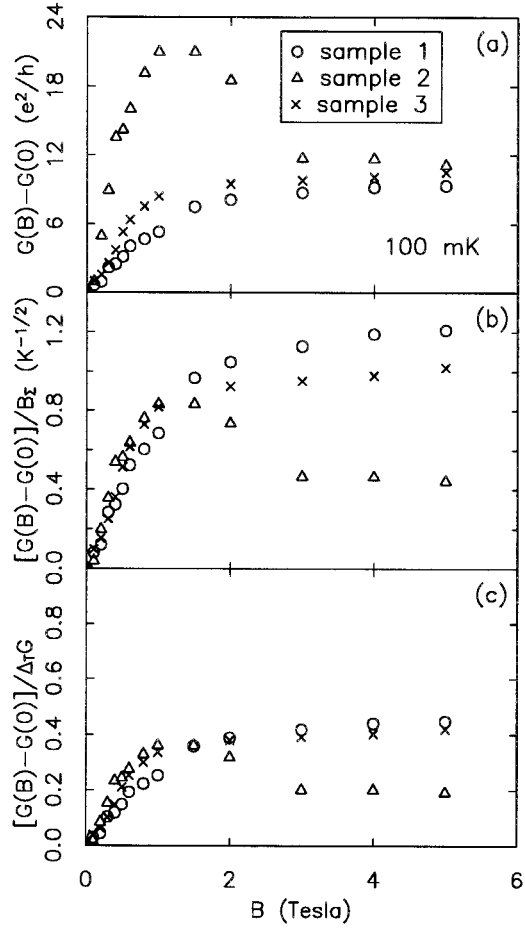

Fig. 14. Magnetic field dependence of the $V=0$ conductance for the 3 unannealed Cu samples at 100 mK. (a) Absolute magnetoconductance. (b) Magnetoconductance scaled by the value of B_{Σ} for each sample. (c) Magnetoconductance relative to the change in conductance between 100 mK and 6 K. An applied magnetic field alters, but does not eliminate, the zero-bias conductance signal due to TLSs.

2 show pure $T^{1/2}$ behavior at $V=0$ (i.e. absence of Δ-corrections) for T as small as 0.4 K. Taking $T_K \approx 5$ K, Eq. (28) implies that for any active TLS, $\Delta < 1.4$ K. This upper bound is rather small, and was discussed at some length in Section V.C.3.

VII. RELATED EXPERIMENTS

In recent years, ZBAs have been found in a number of different nanoconstriction studies [19–21, 54]. It should be appreciated that in each the ZBA could in principle be caused by a different mechanism. However, two recent experiments

have found ZBAs that convincingly seem to be of the same type and origin as those in the quenched Cu constrictions. We review their properties below in the form of a continuation of the list of properties compiled in Section IV, together with their interpretation in terms of the 2CK scenario.

A. *Titanium Nanoconstrictions*

Three of us (ULB) [19] have recently studied nanconstrictions with the same geometry as the quenched Cu constrictions of RB, but with the leads made from Titanium (Ti). This is a stressed refractory metal, which is both more disordered and in a state of higher tensile stress than Cu, and thus is a likely candidate to have dynamical defects. The following properties were found:

(Ti.1) *General properties*: (a) ZBAs occur in more than 90% of the samples. —This high rate of occurence is due to the highly stressed nature of refractory metals (mean free path is estimated to be $l \gtrsim 10\,\text{nm}$),[8] and the consequent abundance of TLSs.

(b) The typical amplitude is about $\Delta G \simeq 10e^2/h$.—This indicates that just a few (probably less than 5) TLSs are involved, since the 2CK model implies a maximum ΔG of $2e^2/h$ per defect (see footnote 2).

(c) The ZBA anneals away at room temperatures on a time scale of a few days to a few months.—This is significantly longer than in Cu samples, because Ti has a higher melting temperature.

(d) *Geometry-induced stress*: If a dirty insulating substrate is used (e.g. with organic contaminants), to which the Ti-film does not stick well, the ZBAs were absent in almost all the samples. The ZBA occurs only if there is good adhesion between metal film and substrate. Nevertheless, the ZBA is *not a surface effect* (e.g. due to TLSs on the surface caused by a mismatch in lattice constants between Ti and the substrate). This was demonstrated as follows by studying constrictions made from a combination of Palladium (Pd) and Ti: Samples made purely from Pd almost never had ZBAs; even when they did, the ZBA annealed away over a period of a few hours, in contrast to the much longer annealing times for Ti (Ti.1c). This implies that stresses are relieved much quicker in Pd than in Ti. Now, for a series of samples, first a layer of Ti of thickness 2, 5, 10 or 25nm was deposited on the both sides of the constriction, and thereafter Pd was used to fill up the bowl and form the leads. If the ZBA were a surface effect, it should have shown up in these samples. However, very few of them had ZBAs, and even when they did, the ZBA annealed away over a period of a few hours, exactly as for the pure-Pd samples. However when the Ti layer's thickness was increased above 30nm, which in these samples is approximately the cross-over thickness for filling the bowl sufficiently to

[8] Note that the mean free path is not much larger (if at all) than the typical constriction radius (5–15 nm). Strictly speaking, this means that one is approaching the regime in which the theory of diffusive, not ballistic, point contact spectroscopy should be used (Section III), but we shall continue to use the latter.

form a continuous nanobridge through the constriction, ZBAs started to appear with annealing times characteristic of Ti. This shows that the ZBA's cause is situated in the bulk of the bowl and not on its surface.

This revealing investigation implies that *the ZBA results from geometry-induced stress in the metal*. This stress is provided by the bowl-like shape of the hole (but only when good adhesion to the bowl is possible) and anneals away very slowly in Ti, but rapidly in Pd. This conclusion strongly supports the assumption (A1) of Section V.D that the ZBA is caused by stress-induced structural defects.

(Ti.2) *V/T scaling*: Some samples show the same scaling behavior, $[G(V, T) - G(0, T)]/T^{\alpha} = F(eV/k_B T)$, as that observed for Cu samples (Cu.9a). Of those samples for which a scaling analysis according to Section VI was done, at least three scale very well for $\alpha \simeq 0.5$; scaling plots for one of these (called sample 4 here) are shown in Fig. 15.—This is in excellent agreement with the 2CK scenario, given assumption (A2) that the TLS energy splittings Δ are sufficiently small. The scaling curve has the same universal shape as for the Cu constrictions (compare with Fig. 8), with the universal number $\Gamma_1 = -0.81 \pm 0.10$ [see Eq. (26) and Table 1], but actually scales better, in that the "bending-down" deviations from scaling occuring in Fig. 8(b) for Cu at large $(V/T)^{1/2}$ are *absent* here. This makes it somewhat hard to unambigously determine the Kondo temperature; estimates give $T_K \simeq 10 - 20$ K.

(Ti.3) *Premature $V^{1/2}$ saturation*: Other samples, such as sample 5 of Fig. 16, show for small T a "premature" saturation of the $V^{1/2}$ behavior, implying a very marked breakdown of scaling. This can be quantified as follows: The conductance (also for sample 4) can be fitted, at fixed T, by the phenomenological form

$$G(V) = G(0) + a[V^2 + (2T_x)^2]^{1/4}, \tag{29}$$

where T_x characterizes the "saturation energy" at which the large-voltage $V^{1/2}$-behavior crosses over to the flat low-V regime. For the scaling sample 4 of (Ti.2) one finds $T_x \simeq T$ [this is the reason for including the phenomenological factor of 2 before T_x^2 in Eq. (29)], meaning sample 4's saturation is due to thermal rounding. In sharp contrast, for sample 5 one finds that for sufficiently low temperatures, T_x ($= 1.43 \pm 0.03$ K) is *much larger* than T (by a factor of almost 20(!) for the lowest T of 76 mK). This implies "premature (non-thermal) saturation" of $V^{1/2}$-behavior as V is lowered. (No such saturation was ever observed in Cu samples down to 50 mK). —The 2CK scenario attributes [see assumption (A2)] premature $V^{1/2}$ saturation to the presence of some TLS with finite energy splittings $\Delta \simeq T_x$. At energies below Δ, 2CK physics "feezes out", and *pure V/T scaling behavior* is destroyed for $(TT_k)^{1/2} < \Delta$ [Eq. (28)], due to the presence of a new energy scale. Note, though, that non-Fermi-liquid physics is destroyed only at low energies—it becomes observable again at sufficiently high energies, as demonstrated by the reemergence of $V^{1/2}$ behavior *above* T_x, in agreement with the last sentence of assumption (A2). Importantly, this implies that even if a constriction contains a large number of impurities with a wide distribution of Δ's, it *can* show $V^{1/2}$ behavior at sufficiently large V, though its

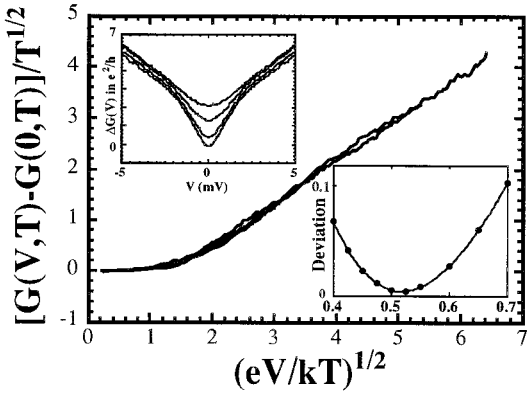

Fig. 15. The differential conductance for a 20Ω Ti constriction (sample 4), for temperatures of 6.0, 4.0, 2.0 and 1.4 K, scales well when plotted in the scaling form $[G(V, T) - G(0, T)]/T^{1/2}$ vs. $(eV/k_B T)^{1/2}$ of Eq. (14) with $\alpha = \frac{1}{2}$ [see (Ti.2)]. Top inset: the unscaled conductance $\Delta G(V) = G(V, T) - G(0, 1.4\text{ K})$. Bottom inset: The deviation parameter $D(\alpha)$ of Eq. (24), which quantifies the quality of scaling, accordance to which $\alpha = 0.52 \pm 0.05$.

scaling will suffer. (Indeed, for the Cu samples the quality of scaling was better (Cu.2) for samples with smaller ZBA amplitudes, i.e. fewer TLSs.)

(Ti.4) *Electromigration*: (a) Electromigration, the application of large voltages ($V = 200$ mV, $J \simeq 10^{10}$ A/cm^2) for short periods of time (10 seconds, several times), can cause significant changes in the saturation energy T_x. For sample 5, Fig. 17(a) shows that T_x changed from 2.3 to 1.4 K as a result of such an electromigration.

(b) Another device (sample 6) had a more complicated low-V behavior [Fig. 17(b)], characterized by a sum of two terms of the form (29), with two distinct saturation energies T_{x1} and T_{x2}. Upon electromigration, they experienced (opposite!) changes, from 0.9 to 1.5 K and 9.7 to 6.8 K, respectively.

Presumably electromigration, which is known to controllably cause defect rearrangement [27, 35], modifies the parameters of some TLSs, thereby changing their Δs. (Ti.4b) is direct evidence that *individual* defects are responsible for the ZBA; evidently, two different TLSs dominate the ZBA in this particular case.

(Ti.5) *Magnetic field*: The magnetic field dependence of $G(V, H)$ is weak and random (see Fig. 18): when H is changed from 0 to 5 T, $G(V, H)$

(a) changes by less than $2e^2/h$, with random sign, for $V < T_x$; and

(b) is completely H-independent for $V > T_x$.

The very weak H-dependence is consistent with 2CK expectations (see Appendix B). It shows that the strong H-dependence observed for Cu ZBAs (Cu.8a) is not a generic property of the ZBA, as discussed in Section V.C.2 and summarized in assumptions (A3, A4). For Ti constrictions, the entire H-dependence can be attributed to *H-tuning of $\Delta(H)$*, i.e. to the fact that in disordered materials, the TLS splitting is known [40, 41] to be a random function $\Delta(H)$ of H due to disorder-enhanced interference effects (see

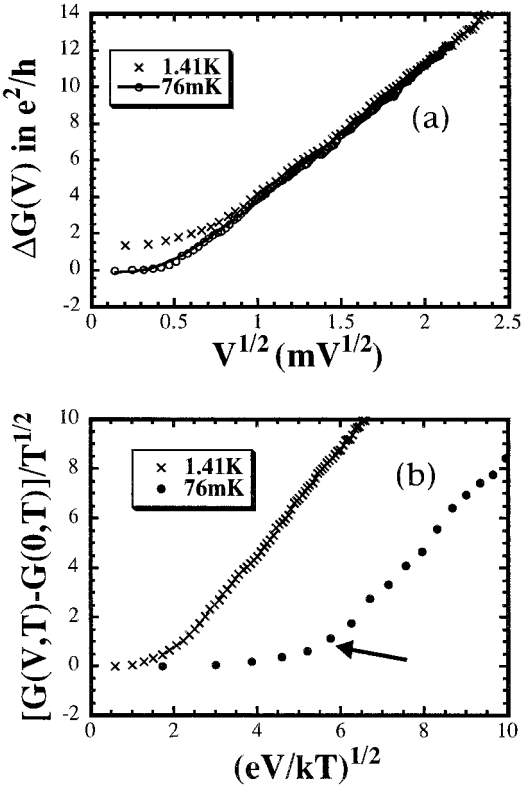

Fig. 16. (a) $\Delta G(V) = G(V, T) - G(0, 0.76\,\mathrm{mK})$ vs. $V^{1/2}$ for a 19Ω Ti construction (sample 5) at 1.41 K and 76 mK. (b) The same data do *not* scale when plotted as $[G(V, T) - G(0, T)]/T^{1/2}$ vs. $(eV/k_B T)^{1/2}$, due to "premature saturation" (see arrow) of the 76 mK curve, as discussed in (Ti.3).

Section V.A.1). H-tuning of $\Delta(H)$ is consistent with the fact that the H-dependent changes in G have roughly the same size (Ti.5a) as those due to changes in Δ induced by electromigration (Ti.4). It explains the random sign of the magneto-conductance (T1.5a), and also explains (Ti.5b), because $\Delta(H)$ can only affect $G(V)$ *below* T_x.

(Ti.6) *No conductance transitions*: The conductance transitions (Cu.9) that occured in at least 80% of the quenched Cu samples have never been observed in any of the Ti samples.—This shows that Cu conductance transitions (Cu.9) are not generic, as discussed in in Section V.C.1 and summarized in Assumption (A3).

The above discussion shows that the Ti nanoconstrictions display all the phenomenology expected from 2CK impurities: (i) their amplitudes are sufficiently small to be attributed to only a very few TLSs; (ii) some of them show good V/T scaling with scaling exponent $\alpha = \frac{1}{2}$; (iii) others demonstrably show the effects of finite, tunable Δ; and (iv) they lack the puzzling conductance transitions and large magnetic field

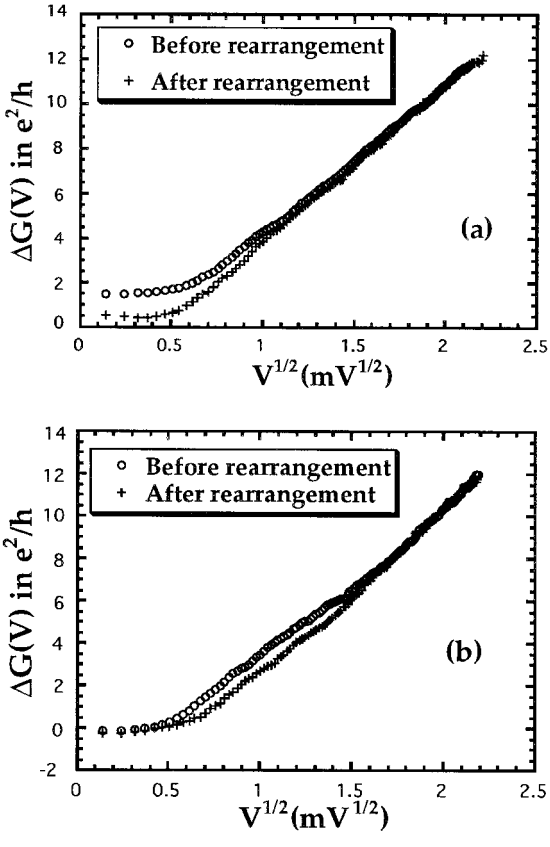

Fig. 17. (a) The ZBA of the Ti sample 5 before and after electromigration [see (Ti.4)], which changed the saturation energy T_x of Eq. (29) from 2.3 to 1.4 K. (b) A 22Ω Ti constriction (sample 6) shows two distinct saturation energies T_{x1} and T_{x2}, which change upon electromigration from 0.9 to 1.5 K and 9.7 to 6.8 K, respectively.

dependence of the quenched Cu samples. Thus, they appear to be "custommade" realizations of 2CK physics in nanconstrictions.

B. *Mechanical Break Junctions Made from Metallic Glasses*

Keijsers, Shklyarevskii and van Kempen [21] studied ZBAs in mechanically controlled break junctions made from metallic glasses, which are certain to contain many TLSs. They observed the following properties:

(MG.1) *Amplitude and shape*: The ZBA has qualitatively exactly the same shape and sign as that of RB's quenched Cu samples, with an amplitude of sometimes more than 100 e^2/h.—The large amplitude is to be expected, since metallic glasses contain a high concentration of TLSs.

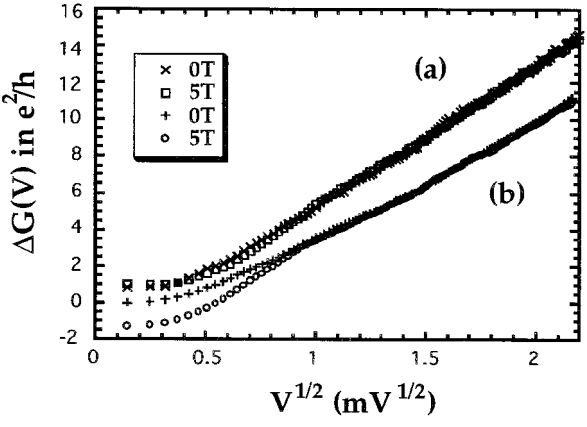

Fig. 18. The magnetic field dependence (at 0 and 5 T) at 100 mK for two Ti constrictions [see (Ti.5)]: (a) sample 5; (b) sample 6. Data for (a) are offset by e^2/h at $V=0$ for clarity.

(MG.2) *Slow ZBA fluctuations*: (a) Remarkably, in some samples the amplitude of their ZBA fluctuates between two values $G(V)$ and $G'(V)$ (or sometimes several) in a telegraph-noise fashion on a time scale of seconds, evidently due to the presence of one (or sometimes several) slow fluctuators (see Section V.A.1) in the constriction region.

(b) The amplitude of these telegraph-fluctuations, $\Delta G(V) = |G - G'|$, is of order $1e^2/h$ or less, *and depends on V*. It decreases from $\Delta G(0)$ to 0 as V increases from 0 to between 5 and 10 mV, see Fig. 19.

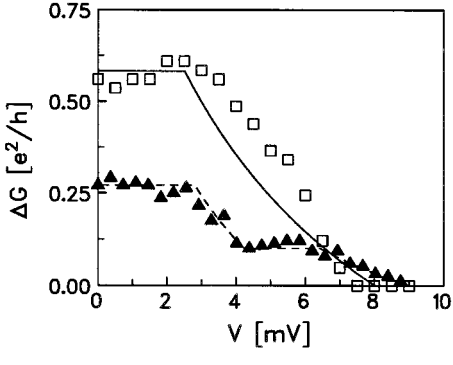

Fig. 19. ZBA fluctuations $\Delta G(V)$ [see (MG.2)] due to the presence of a slow fluctuator in two metallic glass constrictions studied in Ref. [20]. The squares give $\Delta G(V)$ for Fig. 2, curve 3 of [20]; the triangles give the noise amplitude multiplied by 2 (for visibility) of Fig. 4, curve 1 of [20] (uncertainties $\sim 0.1e^2/h$). The fits were obtained in Ref. [56] using VZ's theory to calculate $\Delta G(V)$. For the solid curve a single fast TLS was assumed, experiencing modulations in asymmetry energy between $\Delta_z = 8$ meV and $\Delta'_z = 3$ meV, with $T_K = 17$ K. For the dashed curve two fast TLSs were assumed, with $\Delta_{z1} = 9$, $\Delta'_{z1} = 6.2$ meV, $T_{K1} = 8.9$ K, and $\Delta_{z2} = 4.2$, $\Delta'_{z2} = 2.8$ meV, $T_{K2} = 6.2$ K.

(MG.3) *Magnetic field*: The ZBA shows no H-dependence.—This is exactly as expected in the 2CK scenario (see Section V.C.2), and confirms the conclusion (Ti.5) that the strong H-dependence of Cu ZBAs (Cu.8a) is not a generic property of the ZBA.

(MG.4) *No conductance transitions*: The conductance transitions (Cu.9) of the quenched Cu samples have never been observed metallic-glass constrictions [55].—This confirms the conclusion (Ti.6) that Cu conductance transitions (Cu.9) are not generic.

The V-dependence of $\Delta G(V)$ implies that the large features of the ZBA and the small amplitude fluctuations cannot be unrelated phenomena. For example, it is not possible to attribute the overall ZBA to a suppression in the density of states due to static disorder (analogous to the proposal of WAM for quenched Cu samples, see Appendix A.1), while assuming the additional small conductance fluctuations to be caused by an independent slow fluctuator. The problem with such a scenario would be that the amplitude of the fluctuations, though of the right magnitude of $< e^2/h$, would be *V-in*dependent.

Keijsers *et al.* state that the large features of their ZBA can be explained by invoking either Zawadowski's non-magnetic Kondo model (Section V.A.2) or KK's theory of TLS-population spectroscopy (Appendix A.3) to describe the interaction of electrons with the *fast* TLSs in their system. They propose that the amplitude fluctuations can be explained (in either theory) by assuming that the TLS-electron interaction strengths [V^z and V^x in Eq. (8)] of some fast TLSs are *modulated between two values*, due to short-ranged interactions with a nearby slow two-state system, when the latter hops between its two positions.

Zaránd, von Delft and Zawadowski recently pointed out [56] that the maximum switching amplitudes observed by KSK are so small ($\Delta G_{max} < 1e^2/h$ for all samples in Ref. [21]) that they seem to stem from the parameter-modulations, induced by a slow fluctuator, of only one or two fast TLS, where the parameter expected to be most strongly modulated is the TLS asymmetry energy, which can be assumed to fluctuate between two values, $\Delta_z \Leftrightarrow \Delta'_z$. This implies that the experiments of KSK constitute the first measurements of the conductance contributions of *individual* fast TLSs, and allows an unprecedentedly detailed comparison with theory: by calculating $G(V, \Delta_z)$ (the contribution to the ZBA due to scattering off a TLS with asymmetry energy Δ_z) for various asymmetry energies, it should be possible to find two values Δ_z and Δ'_z for which $|G(V, \Delta_z) - G(V, \Delta'_z)|$ reproduces the measured $\Delta G(V)$.

Analysing two samples in detail, Zaránd, von Delft and Zawadowski showed that $\Delta G(V)$ could not be fit using the TLS-population spectroscopy theory of Kozub and Kulik (Section A.3). However, rather good fits (Fig. 19) were achieved using Zawadowski's non-magnetic Kondo model (although the analysis does not completely rule out that there can be a small KK contribution [56]).

This constitutes possibly the most direct evidence yet for the applicability of the 2CK model to TLS-induced ZBA's in point contacts. Subsequent measurements of the response of such break junctions to RF-irradiation [57] support this conclusion (although they, too, do not completely rule out a small KK contribution). If both

the V- and T-dependence of ΔG were known, a V/T scaling analysis [2] would serve as a further test of the non-magnetic Kondo scenario. (At present the break junctions are not sufficiently stable against mechanical deformations under temperature changes to reliably determine the T-dependence of ΔG.)

VIII. CONCLUSIONS

A. *Summary*

This paper is the first in a series of three (I, II, III) devoted to 2-channel Kondo physics. We have reviewed in detail the experimental facts pertaining to a possible realization of the 2CK model, namely the non-magnetic ZBA in quenched Cu nanoconstrictions, and also integrated into our analysis insights obtained from new experiments on Ti and metallic-glass constrictions.

We have summarized the various experimental facts for the quenched Cu samples in the form of nine properties, (Cu.1) to (Cu.9) (Section IV). Properties (Cu.1–5), which are of a mainly qualitative nature and very robust, place very strong demands on any candidate explanations of the ZBA: the zero-bias anomalies disappear under annealing, and hence must be due to *structural* disorder; they disappear when static disorder is intentionally added, and hence cannot be due to static disorder—instead they must be due to *dynamical* impurities; they show no Zeeman splitting in a magnetic field (Cu.8b), and hence must be of *non-magnetic* origin. These observations lead to the proposal [1] that the zero-bias anomalies are due to nearly degenerate two-level systems, interacting with conduction electrons according to the non-magnetic 2-channel Kondo model of Zawadowski [49], which renormalizes at low energies to the non-Fermi-liquid regime of the 2CK model.

We then presented a quantitative analysis of the V/T scaling behavior of the conductance $G(V, T) = G_o + T^{\alpha} F(eV/k_B T)$, which demonstrates unambigously that the scaling exponent has the unusual value of $\alpha = \frac{1}{2}$, in contrast to the usual Fermi-liquid value of $\alpha = 2$. We argued that this too can naturally be understood within the phenomenology of the $T = 0$ fixed point of the 2CK model, within which the experimental verification of $\alpha = \frac{1}{2}$ constitutes the direct observation of a non-Fermi-liquid property of the system. Breakdown of scaling for larger T and V values is explained too, since for these the system is no longer fine-tuned to be close to the $T = 0$ fixed point, thus spoiling the scaling behavior. Estimates of T_K in the range 1–5 K, which is reasonable, were obtained, as well as an upper bound for the energy splitting of all active TLSs of $\Delta \lesssim k_B 1$ K. This bound is rather small (and has been criticised, see Section V.C.3), but is enforced by the quality of the observed scaling.

The scaling analysis provides sufficiently detailed information about the low-energy physics of the system that it enabled us to rule out several other candidate mechanisms for explaining ZBAs. (An alternative interpretation of the scaling properties recently proposed by Wingreen, Altshuler and Meir can be discounted on other grounds, see Appendix A.1).

We then reviewed experiments on Ti and metallic glass samples in the form of further properties (Ti.1) to (Ti.6) and (MG.1) to (MG.4). They provided further strong support for the 2CK interpretation: the Ti data demonstrated the destruction of scaling in the presence of a non-zero, tunable TLS energy splitting Δ, and the metallic glass data allowed the contribution of a *single* TLS to be measured and compared with theory.

The 2CK interpretation is sufficiently successful in accounting for the observed phenomenology of the scaling properties (Cu.6), that we believe more quantitative calculations based on this model to be justified. The remaining two papers in this series, II and III, are devoted to a quantitative calculation of the scaling function $\Gamma(v)$, to be compared with the experimental curve in Fig. 11(b). The final result is shown in Section V of paper II, Fig. 6. When our results are combined with recent numerical results of Hettler *et al.* [12, 13], quantitative agreement with the experimental scaling curve is obtained.

The main conclusion of this investigation is therefore that *the 2CK interpretation is in qualitative and quantitative agreement with the scaling properties of the data.* It can also account for all other observed properties, with only two exceptions for the quenched Cu samples, summarized below.

B. *Open Questions and Outlook*

There are two experimental observations for the quenched Cu samples that do appear to lie beyond the present understanding of 2CK physics: the conductance transitions (Cu.9) and the apparantly related strong magnetic field dependence (Cu.8a). A theory of this phenomenon would be most welcome. However, these effects appear to involve either "high energy" effects or effects due to interactions between nearly degenerate TLSs which are beyond the scope of the present-day single-impurity calculations of the 2CK model, which are applicable only to the low T- and V-regime in the neighborhood of a $T=0$ fixed point. However, these two experimental effects should not be considered generic to the physics of TLSs in nanoconstrictions: they are absent in metallic-glass and Ti constrictions, and particularly the latter, which display both scaling and the destruction thereof by a non-zero, tunable Δ, seem to be almost "ideal" realizations of 2CK physics.

On the theoretical side, the 2CK model has recently been subjected to renewed scrutiny (catalyzed in part by its application to the ZBA and the claim that non-Fermi-liquid behavior has been observed). The main point of contention is whether any realistic TLS would ever flow towards the non-Fermi-liquid fixed point of the 2CK model, because of the inevitable presence of relevant perturbations that drive the system away from this point.

Wingreen, Altshuler and Meir [15] have argued that static disorder could lead to a significant asymmetry energy Δ between the two states of the TLS (a relevant perturbation). We critically discuss their arguments [15](b), [50] in Appendix D of paper II, and judge them not to be persuasive. More recently, studying a formulation of the model that is slightly different from that introduced by Zawadowski,

Moustakas and Fisher [16] have discovered another relevant operator (which was then interpreted by Zawadowski *et al.* [59] to be due to particle-hole symmetry breaking). However, their conclusions have themselves been questioned in Ref. [59, 60], where the prefactor of this new relevant operator was estimated to be negligably small, and for other technical reasons, some of which are mentioned in Appendix D.2 of paper II.

Certainly, further theoretical work is needed to fully understand the stability, or lack thereof, of the $T=0$ fixed point of the degenerate 2CK model. Both experimental and theoretical work would be welcome to better understand the nature of the defects giving rise to ZBAs in metal point contacts, and the parameters governing these defects. Skepticism of the 2CK interpretation of the data is not unwarranted, since this is seemingly an exotic effect. However, this model has provided a rather complete account of the experimental observations (Cu.1–7), along with accurate predictions of the scaling properties of the conductance signals as a combined function of T and V. No other existing model, based on more familiar physics, has been able to account for all the data.

APPENDIX A: RULING OUT SOME ALTERNATIVE INTERPRETATIONS

In this appendix we discuss a number of conceivable explanations for the ZBA that could come to mind as possible alternatives to the 2CK scenario. We argue that each is inconsistent with some of the experimental facts (Cu.1) to (Cu.9) and hence can be ruled out. Most of this material is contained in [11], [32] and [15]. Nevertheless, since some of these arguments have been the subject of some controversy [15], they deserve to be restated and summarized here, for the sake of completeness and convenience.

1. *Static Disorder*

Could the ZBA be due to static disorder? For example, one could consider attributing the decreased conductance near $V=0$ to either weak localization due to disorder [61] or disorder-enhanced electron-electron interactions [62]. In fact, the latter possibility (first mentioned, but deemed implausible, in Ref. [12]), was recently advocated [15] by Wingreen, Altshuler and Meir (WAM) (these authors also offer a critique [15] of a crucial assumption of the 2CK scenario, which we discussed in Section V.C.3).

WAM made the interesting observation that if just the region of the device near to the point-contact orifice were highly disordered, this would give rise to a local depression in the density of states near the Fermi surface of the form $\delta N(\varepsilon-\varepsilon_F, T) \propto -T^{1/2}F((\varepsilon-\varepsilon_F)/T)$, where F is a scaling function. This in turn would reduce the rate at which electrons incident ballistically into the disordered region could traverse the sample. The total conductance would hence be reduced by an amount $\Delta G(V, T) \propto \partial_V \int_{\varepsilon_F}^{\varepsilon_F+eV} d\varepsilon\, \delta N(\varepsilon-\varepsilon_F, T) = \delta N(V, T)$. Due to the scaling form of δN,

this argument explains the scaling property (Cu.6), and in fact the scaling curve $F(v)$ of Eq. (6) that it produces is in quantitative agreement with that of sample 1 (see [15, Fig. 1]). According to their estimates, this scenario would require a disordered region of diameter 50 nm (the size of the bowl), a mean free path $l = 3$ nm and a diffusion constant $D = 15\ \mathrm{cm}^2/\mathrm{s}$, i.e. rather strong disorder.

The WAM scenario is appealing in that it accounts for the unusual $T^{1/2}$ behavior using well-tested physical ideas, without having to evoke any exotic new physics (such as 2CK non-Fermi liquid physics). However, it is at odds with a number of qualitative (and hence very robust) properties of the ZBA [11, Section 6.6.1], [15, (b)]:

1. According to (Cu.4a), upon the intentional introduction of static disorder the ZBAs are not enhanced, as one would have expected in WAM's static disorder scenario, but *disappear completely*, in contradiction to the latter.

2. The quenched Cu constrictions actually are considerably *cleaner* than is assumed in WAM's scenario, as can be seen from three separate arguments:

(a) According to (Cu.5), a direct estimate of the mean free path, based on the point contact phonon spectrum (a reliable and well-tested diagnostic method [28, 29]) suggests $l \gtrsim 30$ nm instead of WAM's 3 nm.

(b) WAM attempted to explain (Cu.3a), the disappearence of the zero-bias anomalies under annealing, by assuming that the presumed static disorder anneals away at room temperature. However, this suggestion fails a simple quantitative consistency check: let us model the constriction region by a Cu cylinder 40 nm in diameter and 40 nm long, with $l = 3$ nm. Estimating the resistance of this cylinder using the Drude model yields $R = 7\Omega$, which would be the dominant part of the resistance of the device ($R < 10\Omega$ in the lower-R devices). If annealing now removes sufficient disorder that the ZBA disappears, l would have to increase considerably, implying that the overall R of the device would necessarily decrease by tens of percent, which contradicts (Cu.3b) (according to which resistance sometimes even increases under annealing).

(c) According to (Cu.4b) even a somewhat smaller amount of disorder ($l = 7$ nm) than assumed by WAM has been observed to cause voltage dependent conductance fluctuations due to quantum interference. However, these tell-tale signs of static disorder were never seen in the quenched ZBA samples (Cu.4c), though they did appear as soon as disorder was purposefully induced using electromigration (Cu.4b). In other words, in Cu nanoconstrictions the signature of static disorder is conductance fluctuations, not a ZBA.

3. In the static disorder scenario, the conductance depends only on the *average* disorder in the bowl (not on the precise configuration of individual defects). Therefore, it is unclear how to account for the complex behavior of the ZBA under thermal cycling (Cu.3c), under electromigration (Ti.4), and for the V-dependence of the slow ZBA fluctuations $\Delta G(V)$ observed in metallic glass break junctions (MG.2).

Particularly the latter two facts clearly demonstrate that the ZBA strongly depends on *individual* defects.

4. The static disorder scenario predicts a $H^{1/2}$ behavior for the magnetoconductance, and hence is at odds with the very weak H dependence (Ti.5) of the Ti ZBAs.

5. The static disorder scenario provides no hint at all about the possible origin of the conductance transitions. WAM have suggested that these may be due to superconducting regions in the constriction (caused by an attractive electron-electron interaction at short range), but this suggestion fails to account for the presence of several different transitions in the same sample (moreover, superconducitivity in a Cu sample seems highly implausible).

2. *Magnetic Impurities*

The asymptotic dependence of the conductance on $\ln V$ or $\ln T$ (Cu.7) is reminiscent of the magnetic Kondo effect, where the resistance increases as $\ln T$ with decreasing T (as long as $T > T_K$). However, there are at least three strong arguments that rule out magnetic impurities as the source of the anomalies:

1. An effect due to magnetic impurities would not anneal away at higher temperatures (Cu.3a), since magnetic impurities are stable within constrictions, not annealing away at room temperatures over a time scale of 6 months [32].

2. If the magnetic Kondo effect were at work, a magnetic field would cause a well-known Zeeman splitting in the zero-bias conductance dip, as has been observed in nanoconstrictions intentionally doped with the magnetic impurity Mn [11, Section 5.2], as shown in Fig. 4(a). However, in the devices under present consideration, a Zeeman splitting has never been observed (Cu.8b).

3. Magnetic impurities in metal break junctions have been observed to cause ZBAs that do not exhibit splitting because the Kondo temperature scale is larger than the Zeeman energy [63]. However the ZBA signals caused by these impurities are very different than the ones we investigate, because they exhibit Fermi liquid scaling ($\alpha = 2$) rather than the $\alpha = 0.5$ we measure.

3. *TLS Population Spectroscopy*

Many of the qualitative features of the quenched Cu ZBAs can be understood within the framework of Kozub and Kulik's (KK) theory of TLS-population spectroscopy [17, 20], which has recently been extended by Kozub, Rudin, and Schober [18]. This theory assumes that the constriction contains TLSs (labelled by i) with non-zero energy splittings Δ_i, so that the application of a voltage will induce a non-equilibrium population $n_{i\pm}(V)$ of the higher and lower states $|\pm\rangle_i$ of each TLS. Assuming that these two states have different cross-sections $\sigma_i^{\pm}$ for scattering

electrons, the resistance $R(V)$ will then depend non-linearly on the voltage and temperature. According to Kozub and Kulik, the differential resistance has the form

$$\frac{1}{R}\frac{dR}{dV}=\sum_j \frac{eC_j}{2\Delta_j}(\sigma_j^+ - \sigma_j^-)\tanh\left(\frac{1}{2}\tau^{-1}\right) S(v_j, \tau_j, q_j), \tag{A1}$$

where $v_j = eV/\Delta_j$, $\tau_j = k_B T/\Delta_j$, and C_j and q_j are geometrical coefficients depending on the location of the ith TLS in the constriction. The function $S(v, \tau, q)$, which they calculated explicitly, determines the shape of the differential resistance curve (see Fig. 2 of [17]), which can vary quite significantly, depending on the parameters q and τ. Note also that since the signs of $(\sigma_j^+ - \sigma_j^-)$ are arbitrary (except under special assumptions, see [64]), Eq. (A1) predicts that ZBAs of both signs should occur.

The shape of the ZBAs measured by RB is qualitatively the same as that predicted by KK's theory when the latter is averaged over many impurities (KK's theory has significant freedom for curve-fitting, due to the undetermined parameters q_j and Δ_j). However, since the function depends on the two parameters v and τ separately, this theory cannot account for the existance of a scaling law found in (Cu.6a), and certainly not for the specific value $\alpha = \frac{1}{2}$ of the scaling exponent (Cu.6b). Moreover, as pointed out in Section VII, recent related experiments by Keijsers *et al.* [21], in which the behavior of *individual* fast TLSs were probed, shows that they can not be reconciled with KK's theory [56] (see also [57]).

4. *Properties of External Circuit*

It was pointed out to us by G. Schön [65] that fluctuations in the voltage V due to fluctuations in the external circuit can be shown to lead to a conductance $G(V, T)$ that satisfies the V/T-scaling behavior in (Cu.6) (but with the exponent α determined by the external resistance of the circuit, and hence non-universal).

However, since the ZBAs only occur in quenched samples (Cu.1), and since ZBAs anneal away at room temperature (Cu.3a), they must be due to some internal properties of the sample. Hence they cannot be due to properties of the external electrical circuit, such as external voltage fluctations.

5. *Charge Traps and Other Possibilities*

The insulating material used in the devices, namely amorphous Si_3Ni_4, may contain charge traps [66], which could act as Anderson impurities or quantum dots through which conduction electrons could hop. This could cause dips in the differential conductance through several mechanisms, such as Kondo scattering from Anderson impurities [67], inelastic hopping conduction [68, 69] or Coulomb blockade effects [70].

However, charge traps can be ruled out for the present experiments for the following reason. A charge trap has in fact been unambiguously observed in a different

experiment by Ralph and Buhrman [26]. The conductance shows a very characteristic *peak* at $V=0$, in complete contrast to the ZBA-dip. The suggestion of Ref. [26] that this is a Kondo peak that can be associated with Anderson hopping of electrons through the trap was taken up by König *et al.* [71], who calculated the conductance $G(V, T)$ for this scenario and found reasonably good agreement with that experiment. In other words, if charge traps are present, their signals are unmistakable, and very different from the ZBAs of present interest.

Other reasons for ruling out charge traps as causes for the ZBAs may be found in Ref. [11], Section 6.6.2. Also in Ref. [11], Section 6.6, a number of other mechanisms were considered and ruled out as causes for the observed ZBAs: electronic surface states or quasi-localized states within the metal, defect rearrangement, mechanical instabilities, superconducting phases and heating effects.

APPENDIX B: MAGNETIC FIELD DEPENDENCE IN 2CK SCENARIO

It was stated in Section V.C.2 that (contrary to the interpretation we had previously offered in Ref. [2]) 2CK physics is unable to account for the strong magnetic field dependence (Cu.8a) of the ZBA. To illustrate this, we now investigate the two most obvious mechanims through which the 2CK scenario could conceivably produce an H-dependence for the ZBA. These are the H-tuning of the asymmetry energy $\Delta_z(H)$, and channel symmetry breaking. Both drive the system away from the degenerate 2CK fixed point (but not in precisely the same manner), so that H enters as a relevant perturbation. However, we shall conclude that both mechanism are too weak to explain the strength of the observed H-dependence in quenched Cu samples.

1. *H-Tuning of* Δ

One possible mechanism by which H could couple to the system is by tuning [40, 41] the TLS asymmetry energy $\Delta_z(H)$, and hence the energy splitting $\Delta(H)$, which are then random functions of H (see Section V.A.1). With $\Delta(H)$ as a relevant perturbation, the analysis of Section VI.C applies directly, and a correction to the conductance proportional to $\Delta(H)$ can be expected.

However, in this scenario, the magnetoconductance $G(H)$ should be a random function of H (since $\Delta(H)$ is), whereas it seems to be always positive for the samples investigated in more detail. Note also that it would be incorrect to attribute the non-universal non-monotonic features seen at large H for sample #2 to the random behavior of $\Delta(H)$, since closer scrutiny reveals that this behavior is due to the H-motion of the conductance transitions (Cu.9b,v). Moreover, since H-tuning of Δ has its origin in quantum interference, it is expected to occur mainly in strongly disordered environments, which the Cu samples are decidedely not [see (Cu.5)]. Furthermore, it would cause conductance changes of order $2e^2/h$ per TLS

substantially smaller than those observed (Cu.8a) (particularly since the signs of the conductance changes for different TLSs are random, leading to partial cancellations).

Hence, it seems as though H-tuning of Δ is not consistent with the observed H-dependence of the quenched Cu samples.

2. *Channel Symmetry Breaking by H*

The second mechanism by which a magnetic field could affect a 2CK system is Pauli paramagnetism, which *breaks channel symmetry* (recall that the channel index σ refers to the Pauli spin $\uparrow, \downarrow$) by causing a net magnetic moment $M = \mu_B^2 H N(\varepsilon_F)$ [58, Eq. (10.11)]. Any such symmetry-breaking term can in principle give corrections to the critical behavior, and should hence be included in the CFT analysis.

A channel-symmetry breaking field is known to be a relevant perturbation with scaling dimension $-\frac{1}{2}$, (see Eqs. (3.15) of [52]). Hence, in direct analogy to our analysis of the effects of Δ in Section VI.C, it causes a perturbation (to be denoted by $m=3$) to the conductance $G(V, T, H)$, described by Eq. (21) with $\alpha_3 = -\frac{1}{2}$ and $\lambda_3 = \tilde{\lambda}_3 \mu_B |H|/E_3^{1/2}$. Here $\tilde{\lambda}_3$ is a dimensionless number of order unity, and E_3 is an energy that sets the scale at which $|H|$ becomes important. Only the absolute value of H enters, because the model is otherwise symmetric in spin $\uparrow, \downarrow$, so that the sign of the channel-symmetry-breaking field cannot be important.

This correction term in Eq. (21) implies that at a fixed, small temperature T_o and $V=0$, the conductance obeys

$$G(0, T_o, H) - G(0, T_o, 0) \propto |H|. \tag{B1}$$

As was argued in Ref. [2], the available data is at least qualitatively not in contradiction with this prediction, since Fig. 14 shows non-analyticity at $H=0$ and an initial roughly linear behavior (Cu.8a) (note though, that $H^{1/2}$ behavior can not be ruled out either).

What are the effects of channel-symmetry breaking at sufficiently large H? Presumably, the polarization of the Fermi sea will become so strong that one channel of conduction electrons (the one with higher Zeeman energy) will decouple from the impurity altogether, and the system will cross over[9] to the one-channel Kondo fixed point, at which the conductance T-exponent is $\alpha=2$. Hence, at this fixed point the conductance, at fixed, large H, should obey the V/T scaling relation Eq. (14), with $\alpha=2$ [46, Eq. (D29)].

However, it seems unlikely that these considerations of the large-H regime have any relevance at all for the Cu samples, since at large magnetic fields, the conductance transitions have moved into the ZBA-regime (Cu.9b,v), presumably destroying all remnants of universal 2CK physics. (Indeed, a scaling analysis for

[9] The cross-over behavior between the fixed points [e.g. the behavior of $G(0, T, H)$] can not be calculated from CFT, which can only describe the neighborhood of fixed points; it might be possible, though, to calculate this function exactly using Bethe–Ansatz techniques.

sample #2 at fixed $H = 6$ T shows best scaling at neither $\alpha = \frac{1}{2}$ nor 2, but at $\alpha = 0.3$ [32], though this value probably does not have special significance either.)

Having investigated the phenomenology to be expected from channel symmetry breaking, let us now step back and estimate the likely magnitude of this effect. The Pauli paramagnetism that causes channel symmetry breaking merely shifts the *bottom* of the spin-up Fermi sea relative to that of the spin-down Fermi sea by $\mu_B H$, while their respective Fermi-surfaces remain aligned. Therefore, the magnitude of the effect that H has on the Kondo physics near the Fermi surface will be of order $\mu_B H/D$ (where $D \sim \varepsilon_F$ is the bandwidth) and hence negligible. Though this argument is not conclusive (e.g. in poor-man scaling approaches the band-width is renormalized to much smaller values of order $D' = \max[V, T, \Delta]$), it casts serious doubts on the channel-symmetry breaking scenario, in particular because the observed amplitude of the magnetoconductance is by no means small.

Thus, we have to conclude that 2CK physics cannot account for the observed H-behavior (Cu.8a). In Section V.C.2 it was therefore suggested to be linked to the H-motion of the conductance transitions [$V_c(H) \to 0$ as H increases, (Cu.9b,v)].

ACKNOWLEDGMENTS

It is a pleasure to thank B. Altshuler, D. Cox, D. Fisher, S. Hershield, M. Hettler, R. Keijsers, Y. Kondev, V. Kozub, J. Kroha, A. Moustakas, A. Schiller, G. Schön, H. van Kempen, G. Weiss, N. Wingreen, I. Yanson, G. Zaránd, and A. Zawadowski for discussions. This work was partially supported by the National Science Foundation through Award No. DMR-9407245, the MRL Program, Award No. DMR-9121654, and the Cornell MSC DMR 9632275; and by the Office of Naval Research, Award No. ONR N00014-97-I-0142. A.W.W.L. and D.C.R. acknowledge financial support from the A.P. Sloan Foundation. The research was performed in part at the Cornell Nanofabrication Facility, funded by the NSF (Grant ECS-9319005), Cornell University, and industrial affiliates.

REFERENCES

1. D. C. Ralph and R. A. Buhrman, *Phys. Rev. Lett.* **69** (1992), 2118.
2. D. C. Ralph, A. W. W. Ludwig, J. von Delft, and R. A. Buhrman, *Phys. Rev. Lett.* **72** (1994), 1064.
3. D. L. Cox, *Phys. Rev. Lett.* **59** (1987), 1240; *Physica (Amsterdam)* **153-155C** (1987), 1642; *J. Magn. Magn.* **76** & **77** (1988), 53.
4. C. L. Seaman, M. B. Maple, B. W. Lee, S. Ghamaty, M. S. Torikachvili, J.-S. Kang, L. Z. Liu, J. W. Allen, and D. L. Cox, *Phys. Rev. Lett.* **67** (1991), 2882.
5. B. Andraka and A. M. Tsvelik, *Phys. Rev. Lett.* **67** (1991), 2886.
6. D. L. Cox, M. Jarrell, C. Jayaprakash, H. R. Krishna-Murthy, and J. Deisz, *Phys. Rev. Lett. B* **62** (1989), 2188.
7. V. J. Emery and S. Kivelson, *Phys. Rev. B* **46** (1992), 10812; *Phys. Rev. Lett.* **71** (1993), 3701.
8. T. Giamarchi, C. M. Varma, A. E. Ruckenstein, and P. Nozières, *Phys. Rev. Lett.* **70** (1993), 3967.
9. P. Nozières and A. Blandin, *J. Phys. (Paris)* **41** (1980), 193.
10. A. W. W. Ludwig, *Int. J. Mod. Phys. B* **8** (1994), 347.
11. D. C. Ralph, Ph.D. dissertation, Cornell University, 1993.
12. M. H. Hettler, J. Kroha, and S. Hershfield, *Phys. Rev. Lett.* **73** (1994), 1967.

13. M. H. Hettler, J. Kroha, and S. Hershfield, in preparation.
14. J. von Delft, Ph.D. dissertation, Cornell University, unpublished, 1995.
15. (a) N. S. Wingreen, B. L. Altshuler, and Y. Meir, *Phys. Rev. Lett.* **75** (1995), 770. (b) D. C. Ralph, A. W. W. Ludwig, J. von Delft, and R. A. Buhrman, *Phys. Rev. Lett.* **75** (1995), 771; **75** (1995), 2786(E).
16. A. L. Moustakas and D. S. Fisher, *Phys. Rev. B* **53** (1996), 4300; see also condmat/9607208.
17. V. I. Kozub and I. O. Kulik, *Zh. Eksp. Teor. Fiz.* **91** (1986), 2243 [*Sov. Phys. JETP* **64** (1986), 1332].
18. V. I. Kozub, A. M. Rudin, and H. R. Schober, *Solid State Com.* **95** (1995), 415.
19. S. K. Upadhyay, R. N. Louie, and R. A. Buhrman, *Phys. Rev. B* **56** (1997), 12033.
20. R. J. P. Keijsers, O. I. Shklyarevskii, and H. van Kempen, *Phys. Rev. B* **51** (1995), 5628.
21. R. J. P. Keijsers, O. I. Shklyarevskii, and H. van Kempen, *Phys. Rev. Lett.* **77** (1996), 3411.
22. J. M. Maldacena and A. W. W. Ludwig, preprint cond-mat/9502109; *Nucl. Phys. B* **506** (1997), 565.
23. A. Zawadowski, *Phys. Rev. Lett.* **45** (1980), 211.
24. K. Vladár and A. Zawadowski, *Phys. Rev. B* **28** (1983), (a) 1564; (b) 1582; (c) 1596.
25. P. Nozières, *J. Low. Temp. Phys.* **17** (1974), 31.
26. D. C. Ralph and R. A. Buhrman, *Phys. Rev. Lett.* **72** (1994), 3401.
27. K. S. Ralls, Ph.D. dissertation, Cornell University, 1990.
28. A. G. M. Jansen, A. P. van Gelder, and P. Wyder, *J. Phys. C.* **13** (1980), 6073.
29. A. M. Duif, A. G. Jansen, and P. Wyder, *J. Phys.: Cond. Matt.* **1** (1989), 3157.
30. I. K. Yanson and O. I. Shklyarevskii, *Fiz. Nizk. Temp.* **12** (1986), 899 [*Sov. J. Low. Temp. Phys.* **12** (1986), 509].
31. A. A. Lysykh, I. K. Yanson, O. I. Shklyarevskii, and Yu. G. Naydyuk, *Solid State Comm.* **35** (1980), 987.
32. D. C. Ralph and R. A. Buhrman, *Phys. Rev. B* **51** (1995), 3554.
33. A. G. M. Jansen, F. M. Mueller, and P. Wyder, *Science* **199** (1978), 1037.
34. K. S. Ralls and R. A. Buhrman, *Phys. Rev. Lett.* **60** (1988), 2434; *Phys. Rev. B* **44** (1991), 5800.
35. K. S. Ralls, D. C. Ralph, and R. A. Buhrman, *Phys. Rev. B* **40** (1989), 11561.
36. P. A. M. Holweg, J. A. Kokkedee, J. Caro, A. H. Verbruggen, S. Radelaar, A. G. M. Jansen, and P. Wyder, *Phys. Rev. Lett.* **67** (1991), 2549.
37. K. S. Ralls, D. C. Ralph, and R. A. Buhrman, *Phys. Rev. B* **47** (1993), 10509.
38. P. W. Anderson, B. I. Halperin, and C. M. Varma, *Philos. Mag.* **25** (1972), 1; W. A. Phillips, *J. Low Temp. Phys.* **7** (1972), 351.
39. D. L. Cox and A. Zawadowski, preprint cond-mat/9704103; *Advances in Physics*, to appear.
40. N. W. Zimmerman, B. Golding, and W. H. Haemmerle, *Phys. Rev. Lett.* **67** (1991), 1322.
41. G. Golding, N. M. Zimmerman, and S. N. Coppersmith, *Phys. Rev. Lett.* **68** (1992), 998.
42. B. L. Al'tshuler and B. Z. Spivak, *Pis'ma Zh. Eksp. Teor. Fiz.* **49** (1989), 671 [*JETP Lett.* **49** (1989), 772].
43. A. Zawadowski and K. Vladár, *in* "Quantum Tunneling in Condensed Media" (Yu. Kagan and A. J. Leggett, Ed.), p. 427, Elsevier, Amsterdam, 1992.
44. G. Zaránd and K. Vladár, preprint cond-mat/9706091 (1997).
45. A. Muramatsu and F. Guinea, *Phys. Rev. Lett.* **57** (1986), 2337.
46. I. Affleck and A. W. W. Ludwig, *Phys. Rev. B* **48** (1993), 7297.
47. A. C. Hewson, "The Kondo Problem to Heavy Fermions," Cambridge Univ. Press, Cambridge, UK, 1993.
48. K. Vladár, A. Zawadowski, and G. T. Zimànyi, *Phys. Rev. B* **37** (1988), 2001, 2015.
49. G. Zaránd and A. Zawadowski, *Phys. Rev. Lett.* **72** (1994), 542.
50. G. Zaránd and A. Zawadowski, *Physica B* **218** (1996), 60.
51. G. Zaránd and A. Zawadowski, *Phys. Rev. B* **50** (1994), 932.
52. I. Affleck, A. W. W. Ludwig, H.-B. Pang, and D. L. Cox, *Phys. Rev. B* **45** (1992), 7918.
53. We thank A. Zawadowksi for pointing out this argument to us.
54. A. I. Akimenko and V. A. Gudimenko, *Solid State Comm.* **87** (1993), 925.

55. R. J. P. Keijsers, private communication.
56. G. Zaránd, J. von Delft, and A. Zawadowski, to be published in *Phys. Rev. Lett.*; see also the reply by R. J. P. Keijsers, O. I. Shklyarevskii, and H. van Kempen.
57. O. P. Balkashin, R. J. P. Keijsers, H. van Kempen, Yu. A. Kolesnichenko, and O. I. Shklyarevskii, preprint (1997).
58. J. M. Ziman, "Principles of the Theory of Solids," 2nd ed., Cambridge Univ. Press, Cambridge, UK, 1972.
59. A. Zawadowksi, G. Zaránd, P. Noziéres, K. Vladár, and G. T. Zimányi, cond-mat/9706092 (1997).
60. J. Ye, preprint cond-mat/9609076 (1996).
61. G. Bergmann, *Phys. Rep.* **107** (1984), 1.
62. P. A. Lee and T. V. Ramakrishnan, *Rev. Mod. Phys.* **57** (1985), 287.
63. I. K. Yanson, V. V. Fisun, R. Hesper, A. V. Khotkevich, J. M. Krans, J. A. Mydosh, and J. M. van Ruitenbeek, *Phys. Rev. Lett.* **74** (1995), 302.
64. V. I. Kozub and A. M. Rudin, *Physica B* **218** (1996), 64.
65. Though not explicitly stated there, this suggestion follows from results contained in G. Steinebrunner, Diplomthesis, Universität Karlsruhe, 1994; G. Steinebrunner, F. W. J. Hekking and G. Schön, *Physica B* **210** (1995), 420.
66. J. T. Milek, *in* "Handbook of Electronic Materials," Vol. 3, IFI/Plenum, New York, 1971.
67. Y. Meir, N. S. Wingreen and P. A. Lee, *Phys. Rev. Lett.* **70** (1993), 2601.
68. L. I. Glazman and K. A. Matveev, *Ah. Eksp. Teor. Fiz.* **94** (1988), 332 [*Sov. Phys. JETP* **67**(1988), 1276]; *Pis'ma Zh. Eksp. Teor. Fiz.* **48** (1988), 403 [*JETP Lett.* **48** (1988), 445].
69. Y. Xu, A. Matsuda, and M. R. Beasly, *Phys. Rev. B* **42** (1990), 1492; D. Ephron, Y. Xu and M. R. Beasley, *Phys. Rev. Lett.* **69** (1992), 3112.
70. D. V. Averin and K. K. Likharev, *in* "Mesoscopic Phenomena in Solids" (B. L. Altshuler, P. A. Lee, and R. A. Webb, Eds.), Chap. 6, Elsevier, Amsterdam/New York, 1991.
71. J. König, J. Schmidt, H. Schoeller, and G. Schön, *Czech. J. Phys.* **46 S 4** (1996), 2399; preprint cond-mat/9608081; *Phys. Rev. B* **54** (1996), 16820.